

Isotope Effects on Chemical Shifts and Coupling Constants

Cynthia J. Jameson

University of Illinois, Chicago, IL, USA

1	Introduction	1
2	Isotope Shifts: Observations	1
3	Rovibrational Theory of Isotope Shifts	2
4	General Trends in the Electronic Factors	11
5	Isotope Shifts Over Two or More Bonds	11
6	Isotope Effects on Spin–Spin Coupling	13
7	Related Articles	16
8	References	16

1 INTRODUCTION

Where an isotopic label is introduced into a molecule, every neighboring resonant nucleus experiences a slight chemical shift. If the labeling is less than 100%, the resonant nuclei in both the labeled and the unlabeled molecules are observed, with intensities according to statistical distribution. The magnitude of the shift depends on the fractional mass change at the isotope substitution site, on the remoteness of the resonant nucleus from the substitution site, and on the sensitivity of the shielding of the resonant nucleus. Every resonant nucleus in the isotopically labeled molecule experiences this chemical shift due to isotopic substitution, but the shift is only observable under favorable conditions, such as when the shift is larger than the halfwidth of the peaks. Isotope shifts as small as a few ppb have been observed, from zero bonds (the isotopic label itself is the resonant nucleus) to 12 bonds away from the substitution site.^{1–3} When the isotopic label itself is the resonant nucleus, the isotope shift is called a primary isotope shift. Such primary isotope shifts can only be observed indirectly, when two in different molecules are compared. There are also attendant effects on the spin–spin coupling constants in the molecule.⁴ Here, the primary and secondary effects have to be deduced from the proper combination of observed couplings, and it is more appropriate to do this in the reduced coupling constant from which the gyromagnetic ratios have been removed altogether.

Isotope effects on chemical shifts and coupling constants are very important in two distinct ways. First, they have a multitude of practical applications, such as in the determination of molecular structure and the verification of mechanisms of reactions. This is just one more powerful tool in which a very selective tag carries with it the same wealth of information as the chemical shift itself. Second, isotope shifts provide a more stringent test of *ab initio* calculations of chemical shifts in specific molecules, being directly related to the slopes on the shielding surface (a mathematical surface), and, in a more general sense, the trends in the thousands of isotope shifts that have been accumulated^{1–3} provide insight into the general

nature of these shielding surfaces, in terms of the dependence of the details of the surface on the nature of the chemical bond, the net charge of the molecule, bond orders, presence of lone pairs, etc.^{5,6} Isotope effects on coupling constants lack practical applications, but are invaluable from the second point of view. For the most part, coupling constants are obtained in rapidly tumbling systems, and only the isotropic average of the tensor is obtained. The full tensor is very difficult to extract from experiments in oriented molecules, since it is always observed as a sum with the larger dipolar tensor. Since coupling mechanisms other than the Fermi contact mechanism are the ones that give rise to the anisotropy of the tensor, the lack of tensor information leaves us with a severe dearth of critical tests of the *ab initio* calculations. Isotope effects on coupling constants provide additional critical tests, since they depend on the spin–spin coupling surface, not just a single calculated value. The earliest questions asked of theoretical calculations of chemical shifts demanded only that the relative order of chemical shifts be reproduced and that the relative magnitudes agree with experiment. More recently, we have asked how well the calculations reproduce the absolute shielding in specific molecules, not just their relative shifts, and also how well they reproduce the shielding tensor components. These are more stringent tests of theory. In the isotope shift experiments, we ask for even more detailed agreement: how well do the calculations reproduce the shapes of the shielding surfaces as the nuclear coordinates are displaced away from the immediate vicinity of the equilibrium geometry of the molecule? A similar question is posed for the spin–spin coupling surface by the primary and secondary isotope effects on J .

2 ISOTOPE SHIFTS: OBSERVATIONS

We follow the notation introduced by Gombler⁷ for the isotope shift observed for nucleus A upon substitution of the neighboring m' X isotope:

$${}^n\Delta A(m'/m X) = \frac{\nu_A(A^{m'}X\dots) - \nu_A(A^mX\dots)}{\nu_A(A^mX\dots)} (m')m \quad (1)$$

where $\nu_A(A^{m'}X\dots)$ is the resonance frequency of the A nucleus in the molecule having the heavier m' X isotope, which is n bonds away from the observed nucleus. The molecules $(A^{m'}X\dots)$ and $(A^mX\dots)$ are isotopomers. The isotope shift can also be written in terms of the nuclear shielding difference:

$${}^n\Delta A(m'/m X) = \sigma^A(A^mX\dots) - \sigma^A(A^{m'}X\dots) \\ = \sigma - \sigma^* \quad (2)$$

where the asterisk applies to the heavy isotopomer. Just as for spin–spin couplings, this notation becomes ambiguous when A and X are atoms in cyclic compounds in which there are at least two paths connecting the observed nucleus and substituted atom, in which case the observed quantity is an isotope shift corresponding to two or more bond paths.

There are several general observations that have been made about magnitudes and signs of isotope shifts.^{1,8}

1. Upon substitution with a heavier isotope, the NMR signal of the nearby nucleus usually shifts towards lower frequencies (higher shielding). Thus, as defined in equations (1) and (2), isotope shifts are generally negative in sign.
2. The magnitude of the isotope shift depends on how remote the isotopic substitution is from the observed nucleus. Although there are exceptions, one-bond isotope shifts are larger than two-bond or three-bond shifts. In the examples shown in Table 1, there is a clear attenuation of the isotope shift with the number of bonds separating the NMR nucleus and the substitution site.^{9,10}
3. The magnitude of the isotope shift is a function of the observed nucleus, and reflects its chemical shift range. Comparisons can be made in analogous compounds, as in Table 2.
4. The magnitude of the shift is related to the fractional change in mass upon isotopic substitution. The larger the fractional change in mass, $(m' - m)/m'$, the larger the isotope shift, as is obvious in the examples in Table 3. (The signals can be easily assigned according to the abundance of the masses m' and m .) When two different atoms can be substituted in the molecule, the isotopic shifts are commensurate with the fractional change in masses, as in the example in Table 4.
5. The magnitude of the shift is approximately proportional to the number of equivalent atoms that have been substituted by isotopes. In other words, isotope shifts exhibit additivity. When there are multiple equivalent sites and the labeling is less than 100%, the resonant nuclei in the variously labeled and the unlabeled molecules are observed. For example, for a deuterium fraction d (based on the solvent isotopic composition for the exchange), for N equivalent replaceable hydrogens, the statistical limit for the relative intensity of the $\text{XH}_{N-n}\text{D}_n$ isotopomer will be

$$I_n = \frac{N!}{n!(N-n)!} (1-d)^{(N-n)} d^n \quad (3)$$

This strictly statistical formula neglects any isotope effects on the equilibrium constant for the exchange. By doing more than one labeling experiment (using different heavy atom fractions), the identification of the signals with the isotopomers can be unequivocal. Fortunately, in many cases, there is also spin-spin coupling information in the NMR spectrum, so that only one labeling experiment is necessary. When there are several equivalent substitution sites, the additivity of the isotope shifts is obvious, as in the examples in Table 5.¹⁵⁻¹⁸ Deviations from strict additivity are small, and their 0:3:4:3:0 ratio in CH_4 -like systems has been explained.¹⁹ Additivity is observed in long-range isotope shifts as well. For example, the two-bond deuterium-induced isotope shifts of ^{59}Co in hexaamminecobalt(III) chloride are all -5.2 ppm per D in each of the 18 different isotopomers of $[\text{Co}(\text{NH}_3)_6]^{3+}$. Less obvious, but also observed, is the additivity of isotope shifts due to substitution at nonequivalent sites.

Table 1

n	$^n\Delta^{31}\text{P}(^{13}/^{12}\text{C})$ in Ph_3P (ppm)	$^n\Delta^{13}\text{C}(^{2}/^1\text{H})$ in butane-1- d_1 (ppm)
1	-0.0227	-0.298
2	-0.0039	-0.088
3	-0.0018	-0.0291
4	—	+0.0051

Table 2

X	$^1\Delta\text{X}(^{13}/^{12}\text{C})$ (ppm)	Chemical shift range (ppm)
^{77}Se in Me_2Se	-0.228	2200
^{125}Te in Me_2Te	-0.341	3160
^{29}Si	-0.006	600
^{119}Sn	-0.018	3000
^{207}Pb	-1.089	9000
X	$^1\Delta\text{X}(^{18}/^{16}\text{O})$ (ppm)	Chemical shift range (ppm)
^{29}Si	-0.0218	600
^{13}C	-0.019	680
^{31}P	-0.018 to -0.036	950
^{15}N	-0.056, -0.138	1200
^{55}Mn	-0.599	3440
^{99}Tc	-0.22	4500
^{95}Mo	-0.25	7000
^{129}Xe	-0.58	7850
X	$^1\Delta\text{X}(^2/^1\text{H})$ (ppm)	Chemical shift range (ppm)
^{51}V in $[\text{CpVH}(\text{CO})_3]^-$	-4.7	6000
^{93}Nb in $[\text{CpNbH}(\text{CO})_3]^-$	-6.0	5000
^{183}W in $\text{CpWH}(\text{CO})_3$	-10.0	11500

These are the general trends found for all isotope shifts. These general experimental trends provide the testing grounds for the theory of isotope shifts. There are also some tendencies that are less global in nature but that are perceived as correlations in observations of related classes of compounds; for example, one-bond isotope shifts tend to be larger when the bond order between the observed nucleus and the substituted nucleus is higher. These correlations have to be considered separately, since they involve comparisons between different molecules that have many differences other than in the parameters that are being correlated with the isotope shifts.

3 ROVIBRATIONAL THEORY OF ISOTOPE SHIFTS

The effects of intramolecular dynamics (vibration and rotation) on nuclear shielding were theoretically predicted by Ramsey,²⁰ and have been observed in two ways. First, there is an observable temperature dependence of the resonance frequency, even for the 'isolated' molecule (apart from the temperature dependence due to intermolecular interactions). Second, there is an observable shift upon isotopic substitution of neighboring nuclei. Both are effects of differences in averaging over nuclear configuration as the molecule undergoes vibration and rotation.²¹ The temperature dependence of nuclear shielding is observed in the dilute gas phase.²²⁻²⁵ The nuclear shielding in an 'isolated' molecule, $\sigma_0(T)$, is an average of the nuclear magnetic shielding tensor over all possible orientations of the molecule in the magnetic field, and is actually observed as the nuclear shielding in the limit as the pressure approaches zero. One does not extrapolate the results to a true zero pressure, but to a pressure so low that collisional deformation of the molecule no longer contributes to σ , while there are still enough collisions to provide the required rate of transition between vibrational and rotational states. Thus, $\sigma_0(T)$ is an average over all possible rovibrational states of

Table 3

Molecule	m'	m	Isotope shifts (ppm)	Reference
(CH ₃) ₂ CO	3	1	${}^2\Delta$ ${}^{13}\text{C}(3/1\text{H}) = +0.076$	Arrowsmith et al. ¹¹
	2	1	${}^2\Delta$ ${}^{13}\text{C}(2/1\text{H}) = +0.054$	
(CH ₃) ₂ CO	3	1	${}^1\Delta$ ${}^{13}\text{C}(3/1\text{H}) = -0.356$	Arrowsmith et al. ¹¹
	2	1	${}^1\Delta$ ${}^{13}\text{C}(2/1\text{H}) = -0.250$	
CO	17	16	${}^1\Delta$ ${}^{13}\text{C}(17/16\text{O}) = -0.0247$	Wasylishen et al. ¹²
	18	16	${}^1\Delta$ ${}^{13}\text{C}(18/16\text{O}) = -0.0476$	
SeF ₆	76	74	${}^1\Delta$ ${}^{19}\text{F}(76/74\text{Se}) = -0.0154$	Jameson et al. ¹³
	77	74	${}^1\Delta$ ${}^{19}\text{F}(77/74\text{Se}) = -0.021$	
	78	74	${}^1\Delta$ ${}^{19}\text{F}(78/74\text{Se}) = -0.0301$	
	80	74	${}^1\Delta$ ${}^{19}\text{F}(80/74\text{Se}) = -0.0442$	
	82	74	${}^1\Delta$ ${}^{19}\text{F}(82/74\text{Se}) = -0.0576$	

Table 4

Molecule	m'	m	Isotope shift ¹⁴ (ppm)
[CpVH(CO) ₃] ⁻	2	1	${}^1\Delta$ ${}^{51}\text{V}(2/1\text{H}) = -4.7$
	13	12	${}^1\Delta$ ${}^{51}\text{V}(13/12\text{C}) = -0.51$

the molecule, weighted according to the fraction of molecules occupying that state at that temperature.

The average shielding for a given rovibrational state is different for each of several isotopically related species, because the masses enter into the solution of the vibrational–rotational Hamiltonian.²⁶ Thus, the thermal average shielding $\sigma_0(T)$ is different for the isotopomers. These differences are measured as isotope shifts. It is important to know which aspects of isotope shifts are due to dynamical factors (rovibrational averaging of internuclear separations) and which can be attributed to electronic factors (changes in nuclear shielding with bond extension or bond angle deformation). If the theory can sort out the former, isotope shifts can be used to extract the latter, thus providing chemically interesting information that would establish the isotope shift as an easily measurable index of the chemical bond.

3.1 Vibrational Averaging in Diatomic Molecules

The potential energy surface (PES) of a diatomic molecule can be written in terms of a Dunham potential, or more approximately in terms of a Morse potential. The Dunham potential function expresses the potential energy in terms of a Taylor series expansion in $x = (r - r_e)/r_e$:

$$V = a_0x^2(1 + a_1x + a_2x^2 + a_3x^3 + \dots) \quad (4)$$

The potential parameters a_0, a_1, \dots can be obtained from the spectroscopic constants of the molecule. The vibrational levels and functions shown in Figure 1 for the H₂⁺ molecule are typical. The first thing to note is that the anharmonic nature of the potential function leads to an unsymmetrical probability distribution function: there is a higher probability of finding the diatomic molecule extended than compressed. Second, this asymmetry becomes more pronounced as we move up in the potential well. Third, the vibrational levels for D₂⁺ (shown also as dashed lines) lie lower in the potential well than those for H₂⁺, corresponding to its lower vibrational frequency,

$\omega_e = 1643.0 \text{ cm}^{-1}$ for D₂⁺ compared with 2323.5 cm^{-1} for H₂⁺. Since we are interested in vibrational averaging and the mass dependence of shielding, we show in Figure 2 the vibrational functions of D₂⁺ and H₂⁺. It is obvious that the anharmonic potential will give rise to different vibrational averages for the isotopomers, since the more sharply peaked and compact probability density of D₂⁺ should lead to a different average than that for H₂⁺, in which the probability density is more spread out at the larger separations. This is true for the vibrational ground state, and the differences become even more pronounced at higher vibrational levels. The average values $\langle x^n \rangle$ can be obtained. Complete calculations for some isotopomers of H₂⁺ lead to the results for the ground vibrational state shown in Table 6, which also shows the results for the case where the vibration is truly that of a harmonic oscillator (HO).

In order to observe more easily the largest terms that contribute to the above equations and explicitly express their mass dependence, we write only the leading terms, expressed in the measured spectroscopic constants of the molecule.⁸

$$\langle x \rangle_{vJ} = -3(v + \frac{1}{2})a_1 \frac{B_e}{\omega_e} + 4J(J+1) \frac{B_e}{\omega_e^2} \quad (5)$$

$$\langle x^2 \rangle_{vJ} = 2(v + \frac{1}{2}) \frac{B_e}{\omega_e} \quad (6)$$

Of these quantities, a_1 is mass-independent, and the others depend on the reduced mass of the diatomic molecule as follows:

$$\omega_e^* = \left(\frac{\mu}{\mu^*}\right)^{1/2} \omega_e, \quad B_e^* = \frac{\mu}{\mu^*} B_e \quad (7)$$

Furthermore, the thermal average $\langle v + \frac{1}{2} \rangle^T$ is also mass-dependent, since the populations of the vibrational energy levels over which this average is taken depend on the vibrational frequency ω_e . Note that B_e/ω_e^2 is mass-independent, so the rotational contribution to the thermal average shielding in the diatomic molecule is independent of mass.

Note also that if we include only the leading terms then

$$\langle x \rangle_v = -\frac{3}{2}a_1 \langle x^2 \rangle_v \quad (8)$$

The difference between two isotopomers is

$$\langle x^2 \rangle_{vJ} - \langle x^2 \rangle_{vJ}^* = 2 \frac{B_e}{\omega_e} \left[1 - \frac{\mu}{\mu^*} \right]^{1/2} (v + \frac{1}{2}) + \dots \quad (9)$$

Table 5

	Isotopomer	δ , observed (ppm)	δ , if exactly additive (ppm)	Deviation (ppm)
^{119}Sn	SnH_3^-	0.0	0.0	0
	SnH_2D^-	-3.093	-3.108	-0.015
	SnHD_2^-	-6.202	-6.217	-0.015
	SnD_3^-	-9.325	-9.325	0
^{119}Sn	SnH_4	0.0	0.0	0
	SnH_3D	-0.4266	-0.4026	+0.024
	SnH_2D_2	-0.8369	-0.8052	+0.032
	SnHD_3	-1.2306	-1.2077	+0.023
	SnD_4	-1.6103	-1.6103	0
^{31}P	PH_3	0.0	0.0	0
	PH_2D	-0.8045	-0.8458	-0.041
	PHD_2	-1.6491	-1.6916	-0.042
	PD_3	-2.5373	-2.5373	0
^{15}N	NH_3	0.0	0.0	0
	NH_2D	-0.6264	-0.6229	0.0035
	NHD_2	-1.2491	-1.2458	0.0033
	ND_3	-1.8687	-1.8687	0
^{15}N	NH_4^+	0.0	0.0	0
	NH_3D^+	-0.3077	-0.2933	+0.0144
	NH_2D_2^+	-0.6048	-0.5865	+0.0183
	NHD_3^+	-0.8937	-0.8798	+0.0139
	ND_4^+	-1.1730	-1.1730	0
^{13}C	CH_4	0.0	0.0	0
	CH_3D	-0.2016	-0.19865	+0.003
	CH_2D_2		-0.3973	
	CHD_3	-0.6006	-0.5960	+0.004
	CD_4	-0.7946	-0.7946	0

$$\langle x \rangle_{vJ} - \langle x \rangle_{vJ}^* = -3a_1 \frac{B_e}{\omega_e} \left[1 - \left(\frac{\mu}{\mu^*} \right)^{1/2} \right] \left(v + \frac{1}{2} \right) + \dots \quad (10)$$

The leading term in $\langle x^3 \rangle_{vJ}$ has the same mass dependence as the next higher order term in $\langle x \rangle$ and $\langle x^2 \rangle$; thus, it is consistent to include only the above two terms. We find the ratios from the full calculations:

$$\frac{\langle x \rangle_{\text{H}_2^+} - \langle x \rangle_{\text{HT}^+}}{\langle x \rangle_{\text{H}_2^+} - \langle x \rangle_{\text{HD}^+}} = 1.370 \quad (11)$$

$$\frac{\langle x^2 \rangle_{\text{H}_2^+} - \langle x^2 \rangle_{\text{HT}^+}}{\langle x^2 \rangle_{\text{H}_2^+} - \langle x^2 \rangle_{\text{HD}^+}} = 1.369 \quad (12)$$

whereas using *only* the leading terms leads in both cases to the ratio

$$\frac{1 - (\mu_{\text{H}_2^+}/\mu_{\text{HT}^+})^{1/2}}{1 - (\mu_{\text{H}_2^+}/\mu_{\text{HD}^+})^{1/2}} = 1.370 \quad (13)$$

Qualitatively, the mass change accompanying the replacement of ^mX by its heavier isotope $^{m'}\text{X}$ leads to a shorter average

bond length. In Figure 2, we show for the lowest vibrational levels the probabilities of finding the diatomic molecule at the various internuclear separations. For the same anharmonic potential, the lighter isotopomer H_2^+ clearly shows greater probabilities of being found in a more extended configuration compared with D_2^+ at each vibrational state. Since the vibrational frequencies are lower for the heavier isotopomer, the populations of its higher vibrational states are somewhat greater. Both effects constitute the mass dependence of the thermal average $\langle x \rangle^T$, with the latter being less important than the former:

$$\{ \langle x \rangle^T - \langle x \rangle^{*T} \} \approx -3a_1 \frac{B_e}{\omega_e} \left[1 - \left(\frac{\mu}{\mu^*} \right)^{1/2} \right] \left(v + \frac{1}{2} \right)^T \quad (14)$$

If we use a harmonic oscillator density of vibrational states, we get a simple form

$$\left(v + \frac{1}{2} \right)_{\text{HO}}^T = \frac{1}{2} \coth(hc\omega_e/2k_B T) \quad (15)$$

which itself has a mild mass dependence, which is not too important when ω_e is large, in which case $\coth(hc\omega_e/2k_B T)$

Table 6

$x = (r - r_e)/r_e$	H_2^+	HD^+	HT^+	D_2^+
$\langle x \rangle_{v=0}$	0.033 12	0.028 63	0.026 97	0.023 32
$\langle x^2 \rangle_{v=0}$	0.014 47	0.012 35	0.011 58	0.009 90
$\langle x^3 \rangle_{v=0}$	0.001 66	0.001 24	0.001 09	0.000 81
$\text{HO } \langle x \rangle_v, \langle x^3 \rangle_v$	0	0	0	0
$\text{HO } \langle x^2 \rangle_{v=0}$	0.012 98	0.011 24	0.010 598	0.009 178
$\omega_e \text{ (cm}^{-1}\text{)}$	2323.5	2012.2	1897.2	1643.0

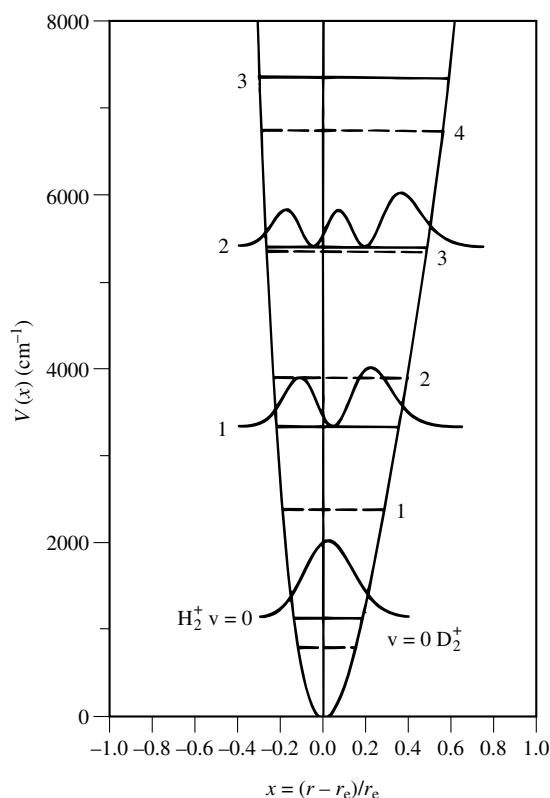


Figure 1 Vibrational levels and wavefunctions (squared) for the H_2^+ molecule. Also shown, by dashed lines, are the vibrational levels of the D_2^+ molecule

is very close to 1. A useful form of an approximate potential for the diatomic molecule is the Morse function

$$V = D_e \{1 - \exp[-a(r - r_e)]\}^2 \quad (16)$$

where D_e is the dissociation energy and a is called the Morse parameter, ar_e being a dimensionless quantity related to the ratio

$$\frac{1}{3!} \left(\frac{d^3 V}{dx^3} \right)_e \bigg/ \frac{1}{2!} \left(\frac{d^2 V}{dx^2} \right)_e = -ar_e = a_1 \quad (17)$$

and

$$\langle x \rangle = \frac{3}{2} ar_e \langle x^2 \rangle \quad (18)$$

At this level of theory, the mass dependence of $\langle x^2 \rangle$ is the same as that of $\langle x \rangle$. Thus, we find that for diatomic molecules, neglecting the mass dependence in the coth function,

$$\begin{aligned} \langle x \rangle^T - \langle x \rangle^{*T} &\approx \frac{3ar_e B_e}{2 \omega_e} \left[1 - \left(\frac{\mu}{\mu^*} \right)^{1/2} \right] \coth \left(\frac{hc\omega_e}{2k_B T} \right) \\ &\approx \langle x \rangle^T \left[1 - \left(\frac{\mu}{\mu^*} \right)^{1/2} \right] \end{aligned} \quad (19)$$

or

$$\langle \Delta r \rangle^T - \langle \Delta r \rangle^{*T} \approx \langle \Delta r \rangle_{\text{vib}}^T \left[1 - \frac{\mu}{\mu^*} \right]^{1/2} \quad (20)$$

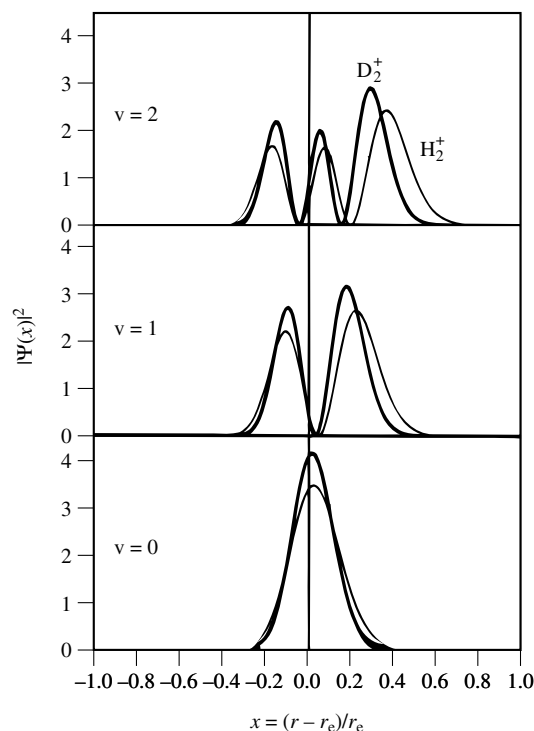


Figure 2 Vibrational wavefunctions (squared) for the D_2^+ molecule (heavy lines) and the H_2^+ molecule (light lines)

$$\langle \Delta r \rangle_{\text{vib}}^T \approx \frac{3ar_e^2 B_e}{2 \omega_e} \coth \left(\frac{hc\omega_e}{2k_B T} \right) \quad (21)$$

When μ/μ^* is very close to 1 (which is true for most situations not involving hydrogen), $1 - (\mu/\mu^*)^{1/2}$ can be further approximated by $(\mu^* - \mu)/2\mu^*$ or, in the comparison of the isotomers A^mX and $\text{A}^{m'}\text{X}$, by²⁷

$$1 - \left(\frac{\mu}{\mu^*} \right)^{1/2} \approx \frac{1}{2} \frac{(m' - m)}{m'} \frac{m_A}{(m_A + m)} \quad (22)$$

$$\langle \Delta r \rangle^T - \langle \Delta r \rangle^{*T} \approx \langle \Delta r \rangle_{\text{vib}}^T \frac{1}{2} \frac{(m' - m)}{m'} \frac{m_A}{(m_A + m)} \quad (23)$$

with an analogous expression for $\langle (\Delta r)^2 \rangle$. Here we find already the origin of general trend 4 in Section 2. The dynamic factors contain the mass dependence, and in diatomic molecules this mass dependence takes a simple form. It is interesting to point out here that, even for polyatomic molecules, this mass dependence has been found to hold: for $m'/m\text{SeF}_6$, a plot of $\langle \Delta r_{\text{SeF}} \rangle^T$ and $\langle (\Delta r_{\text{SeF}})^2 \rangle^T$ versus $(m' - m)/m'$ for $m = 74$ and $m' = 76, 77, 78, 80, 82$ leads to straight lines passing through the origin.²⁸

A very interesting global description of potential functions for diatomic molecules was given by Herschbach and Laurie.²⁹ They found that the second and third derivatives of the potential could be described by exponential functions of the equilibrium internuclear distance, each described by a family of curves which are determined by the locations of the bonded atoms in rows of the Periodic Table:

$$\langle \Delta r \rangle^n F_n \approx 10^{-(r_e - p_n)/q_n} \quad (24)$$

where

$$F_3 \equiv \frac{1}{3} \left(\frac{d^3 V}{dr^3} \right)_e, \quad F_2 \equiv \left(\frac{d^2 V}{dr^2} \right)_e \quad (25)$$

and p_n and q_n are parameters that characterize any two rows of the Periodic Table. It was proposed by Jameson and Osten²⁷ that the averages $\langle x \rangle_v$ and $\langle x^2 \rangle_v$ can be determined entirely from a knowledge of the r_e and the rows of the Periodic Table to which the atoms belong, using the following relations:

$$\langle \Delta r \rangle_v = r_e \langle x \rangle_v \approx \frac{3h}{8\pi} \mu^{-1/2} 10^{-D} (2v+1) \quad (26)$$

$$\langle (\Delta r)^2 \rangle_v = r_e^2 \langle x^2 \rangle_v \approx \frac{h}{4\pi} \mu^{-1/2} 10^{-d} (2v+1) \quad (27)$$

where

$$D \equiv \frac{r_e - p_3}{q_3} - \frac{3(r_e - p_2)}{2q_2} \quad (28)$$

$$d \equiv \frac{r_e - p_2}{2q_2} \quad (29)$$

Figure 3 shows a plot of $\langle \Delta r \rangle_{\text{vib}}$ calculated at 300 K for a large set of diatomic molecules using their individual spectroscopic constants. It appears that the global relation given in equation (26) provides a reasonably good description of the vibrationally averaged bond displacement for diatomic molecules. It has been shown that these equations can be used as well to estimate the dynamic parts for polyatomic molecules, except that the constant factor is closer to $\frac{3}{7}$ than $\frac{3}{8}$.

3.2 The Shapes of Shielding Surfaces

In the context of the Born–Oppenheimer approximation, analogous to the potential energy surface, which is a mass-independent electronic property of a molecule in a given electronic state, there is likewise a mass-independent nuclear shielding surface that describes the variation of the shielding as a function of nuclear configuration. For a diatomic molecule, this surface can be described entirely in terms of the internuclear separation. Two examples are shown in Figures 4 and 5. At the united atom limit ($r = 0$), the diamagnetic shielding of the He^+ ion is (not shown) 35.5009 ppm. At the equilibrium geometry of H_2^+ , the proton shielding is 11.4296 ppm, and at the separated atom limit, the diamagnetic shielding corresponds to half that of the free hydrogen atom ($\frac{1}{2}$) 17.75 ppm.³⁰ The other example is ^{23}Na shielding in NaH, in which the shielding at the equilibrium geometry is lower than for the separated system (either Na^+ or Na atom).³¹ Figure 4 is a typical shielding surface for diatomic molecules in that the shielding surface has negative first and second derivatives.^{32,33} For example, ^{19}F in the HF molecule and in the F_2 molecule, and ^{35}Cl in the HCl molecule and in the ClF molecule, all have negative first and second derivatives; that is, deshielding accompanies bond extension. It is also typical for the proton shielding in the molecule at its equilibrium geometry to be greater than that for the free H atom in the separated systems. On the other hand, the heavy nuclei

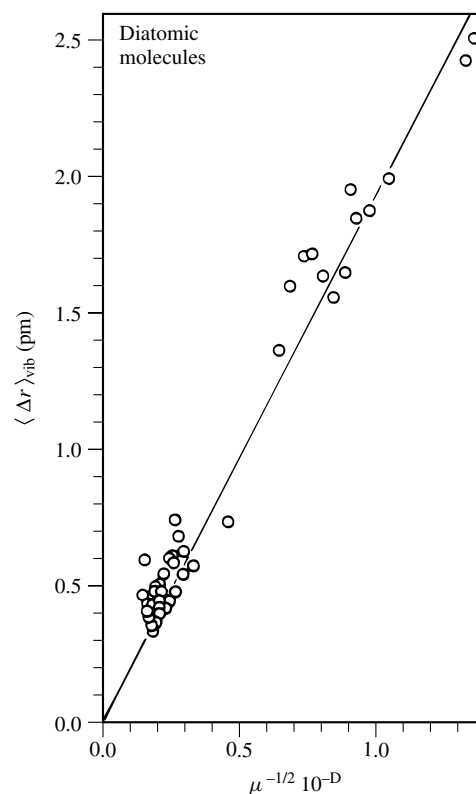


Figure 3 Mean bond displacement in diatomic molecules calculated by vibrational averaging over their individual potential surfaces compared with the global form $\langle \Delta r \rangle_{\text{vib}} \approx (3h/8\pi) \mu^{-1/2} 10^{-D}$ (the straight line), where D is defined in equation (28). (Reproduced by permission of the American Institute of Physics from Jameson and Osten²⁷)

are generally deshielded in the molecule at its equilibrium geometry compared with the diamagnetic shielding of the free atom. For example, nearly all ^{19}F nuclei have shielding less than 470.71 ppm. (^{19}F in ClF is a notable exception, and ^{19}F in CH_3F has an isotropic shielding nearly the same as that of the free F atom.) Every ^{19}F shielding first derivative at the equilibrium geometry, including ^{19}F in the ClF molecule, has been found to be negative, and the second derivative is negative as well.³⁴ On the other hand, the shielding surfaces for ^{23}Na in NaH and ^7Li in LiH have positive first derivatives at the equilibrium geometry.³¹ The shapes of the shielding surfaces in Figures 4 and 5 are fairly similar; the major difference is which point on the shielding surface corresponds to the pocket in the PES and to which side of the shielding minimum this point corresponds. We have seen that the general behavior in vibrational averaging in the anharmonic PES is that the probabilities are greater on the $r > r_e$ side. Thus, dynamic averaging always leads to deshielding when the pocket in the PES is to the short- r side of the shielding minimum, whereas dynamic averaging leads to increased shielding relative to the shielding at the equilibrium geometry when the pocket in the PES is to the longer- r side of the shielding minimum. Most nuclei that are observed in NMR are found on the right-hand side of the Periodic Table, where the shielding surface and the PES are related as in Figure 4; there are fewer observations of the alkali and alkaline earth nuclei, whose shielding surfaces and PES are related as in Figure 5. Therefore, the usual case

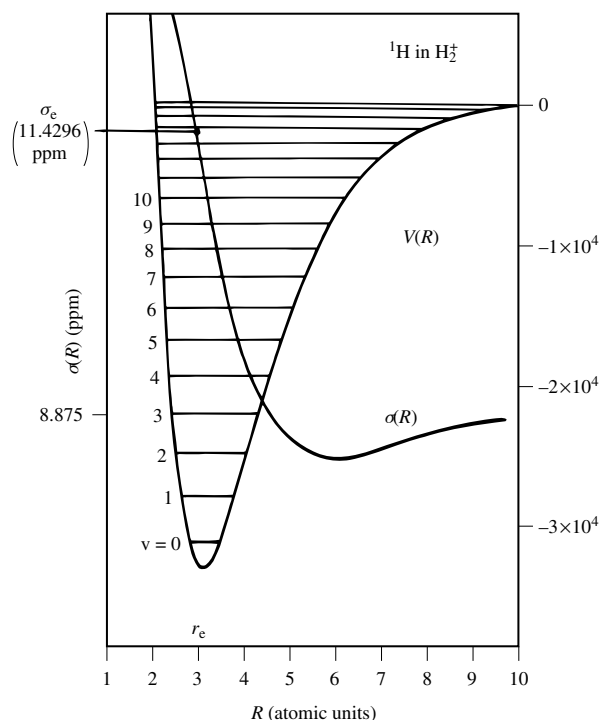


Figure 4 The ^1H shielding surface for the H_2^+ molecule is shown with the potential energy surface. The shielding surface is from ab initio calculations by Hegstrom.³⁰ (Reproduced by permission of the American Institute of Physics from Jameson and de Dios³¹)

is more like Figure 4. Here then is the explanation for general trend 1 in Section 2: superposition of Figure 2 on Figure 4 would lead to a nucleus in the lighter isotopomer being less shielded than the same nucleus in the heavy isotopomer. Preponderance of this situation would lead to a nearly universal sign of one-bond isotope shifts. The exceptions will be Li and Na in the hydrides, for example.

The magnitudes of the isotope shifts would correspond to the ranges of chemical shifts of the observed nucleus if the shielding surfaces themselves scale to these. Let us see. We present the shielding surfaces in the vicinity of the equilibrium geometry in analogous compounds in Figure 6, where ^{19}F in F_2 is compared with ^{35}Cl in ClF (both are bonded to fluorine). ^{19}F in HF is compared with ^{35}Cl in HCl (both are bonded to an H atom). Finally, ^{23}Na in NaH is compared with ^7Li in LiH . It is found that if the change in shielding, $\sigma(r) - \sigma(r_e)$, is scaled by the factor $r_e(a_0^3/r^3)$, the equilibrium bond distance in the molecule and the purely electronic quantity $\langle a_0^3/r^3 \rangle$ characteristic of the atom, for the observed nucleus, the surfaces that describe the change in the shielding of different nuclei in analogous bonding situations superimpose.³¹ This then is an explanation for general trend 3 in Section 2: the magnitude of the isotope shift is a function of the observed nucleus and reflects its chemical shift range. A general discussion of shielding surfaces is given by de Dios and Jameson.³⁵

3.3 Averaging Over Shielding Surfaces

It is sometimes actually necessary to evaluate the average over a large part of the shielding surface.³⁶ For example, the

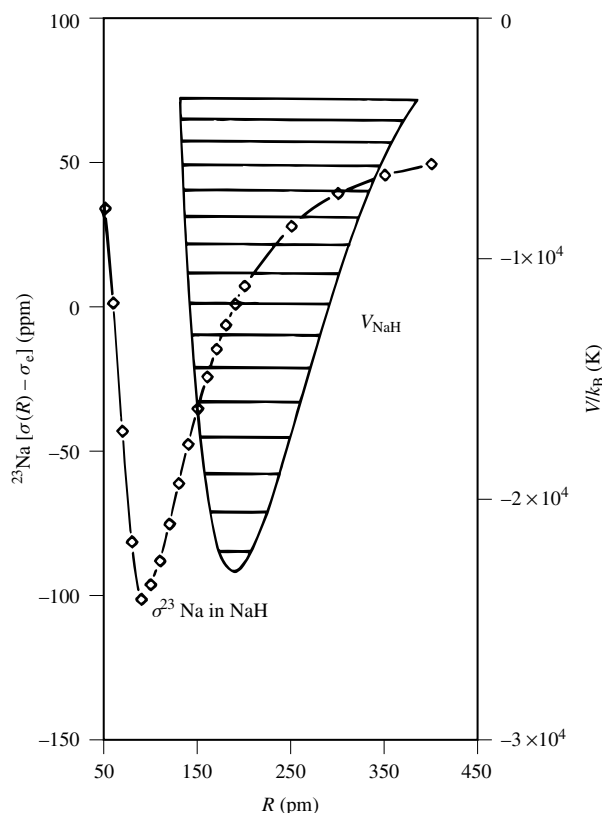


Figure 5 The ^{23}Na shielding surface for the NaH molecule is shown with the potential energy surface. The shielding surface is from ab initio calculations by Jameson and de Dios. (Reproduced by permission of the American Institute of Physics from Jameson and de Dios³¹)

PES of the NH_3 molecule has a rather broad double minimum in the inversion coordinate. The trace on the ^{15}N shielding surface along this inversion coordinate is shown in Figure 7. To obtain the contribution to the average ^{15}N shielding from this degree of freedom, it was necessary to find the numerical PES (which are highly anharmonic) and solve for the vibrational wavefunctions. These are shown in Figure 7. The average for each state 0^s , 0^a , 1^s , 1^a , 2^s , 2^a was numerically calculated with these functions, $\langle \Psi_v | \hat{\sigma} | \Psi_v \rangle$, and the thermal average is obtained as

$$\langle \sigma \rangle^T = \frac{\sum_v e^{-E_v/k_B T} \langle \sigma \rangle_v}{\sum_v e^{-E_v/k_B T}} \quad (30)$$

For semirigid molecules that we often observe in NMR (excluding molecules that are fluxional or that undergo low-frequency torsion), the motions involved in the averaging take place in a small pocket of the potential energy surface close to the equilibrium configuration. It is therefore not necessary to calculate the entire shielding surface, as we have shown in Figures 4, 5, and 7. In the same way that averages such as $\langle x \rangle$, $\langle x^2 \rangle$, $\langle x^3 \rangle$, etc. could be evaluated in terms of the derivatives of the PES such as represented by the quantities a_0 , a_1 , a_2 , a_3 , etc. in the Dunham potential function, it is possible to calculate the average shielding from derivatives of the shielding surface at the equilibrium geometry, since we only need to average over very small displacements away from the minimum in the PES.

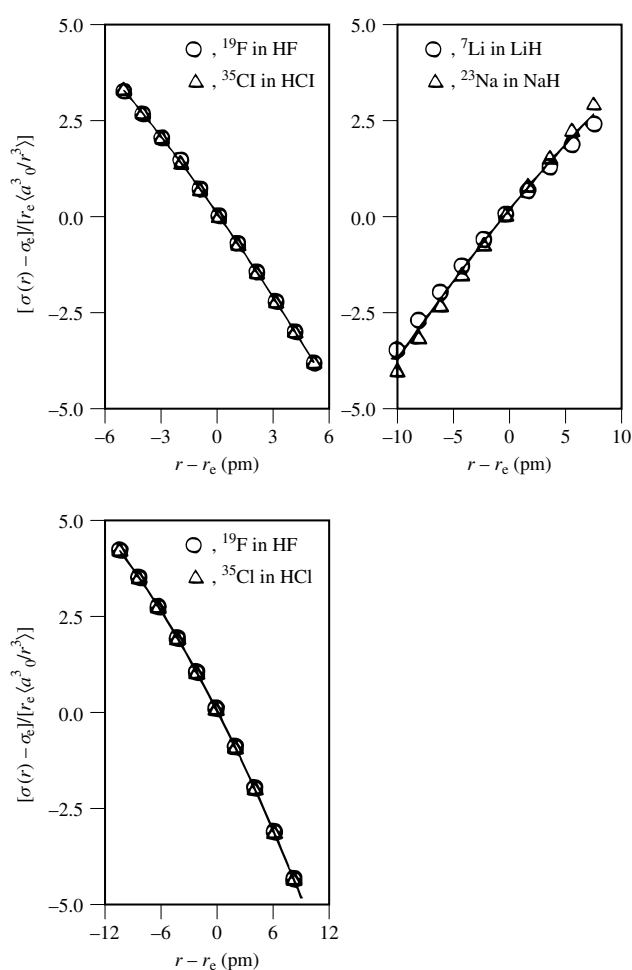


Figure 6 The shielding surfaces of analogous diatomic molecules in the vicinity of the equilibrium geometry, in the range of nuclear displacements spanning the classical turning points of the ground vibrational state. (Reproduced by permission of the American Institute of Physics from Jameson and de Dios³¹)

For a diatomic molecule, it is convenient to expand the shielding surface as a power series in $x = (r - r_e)/r_e$. For a particular molecular state characterized by vibrational and rotational quantum numbers v and J ,

$$\langle \sigma \rangle_{vJ} = \sigma_e + \left(\frac{d\sigma}{dx} \right)_e \langle x \rangle_{vJ} + \frac{1}{2} \left(\frac{d^2\sigma}{dx^2} \right)_e \langle x^2 \rangle_{vJ} + \dots \quad (31)$$

Here $\langle x \rangle_{vJ}$, $\langle x^2 \rangle_{vJ}$, ... are the averages over the vibrational-rotational wavefunctions corresponding to the (v, J) level, which we have already described in Section 3.1. The isotope shift is therefore given by

$$\begin{aligned} \langle \sigma \rangle^T - \langle \sigma \rangle^{*T} &= \left(\frac{d\sigma}{dx} \right)_e (\langle x \rangle^T - \langle x \rangle^{*T}) \\ &+ \frac{1}{2} \left(\frac{d^2\sigma}{dx^2} \right)_e (\langle x^2 \rangle^T - \langle x^2 \rangle^{*T}) + \dots \end{aligned} \quad (32)$$

With the approximations described in Section 3.1, using the Morse parameter,

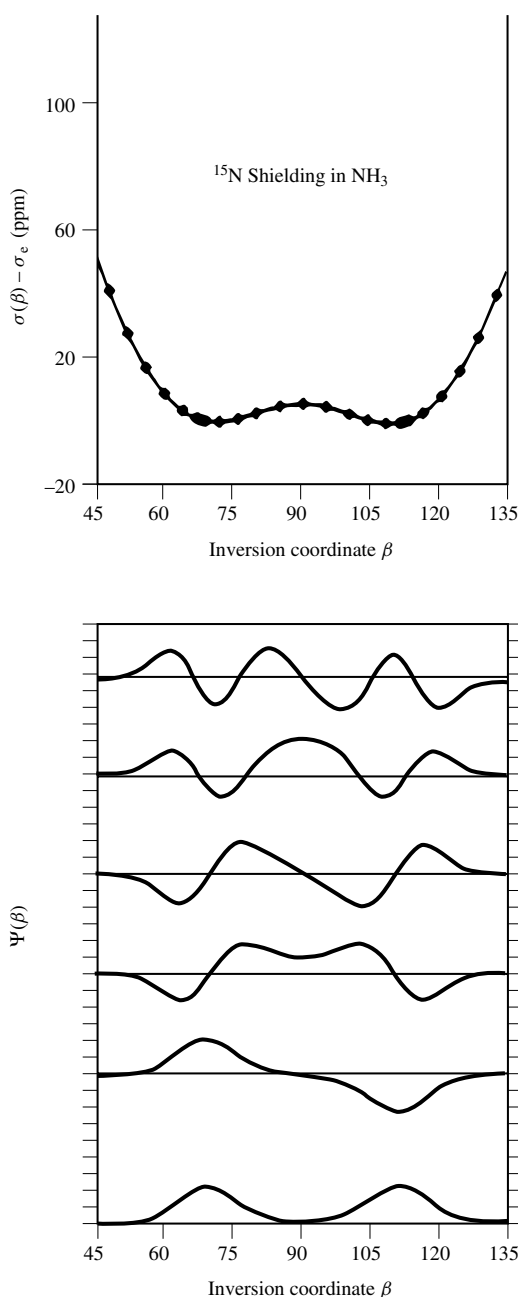


Figure 7 The ^{15}N shielding surface of NH_3 along the inversion coordinate β (the angle between the symmetry axis and a N–H bond) is shown with the vibrational wavefunctions for the lowest inversion levels. The shielding average can be obtained by numerical integration as $\langle \sigma \rangle_v = \int \Psi_v^*(\beta) \sigma(\beta) \Psi_v(\beta) d\beta$. (Reproduced by permission of the American Institute of Physics from Jameson et al.³⁶)

$$\langle x \rangle^T \approx \frac{3}{2} a r_e \langle x^2 \rangle^T \quad (33)$$

the isotope shift in diatomic molecules is given by

$$\begin{aligned} \langle \sigma \rangle^T - \langle \sigma \rangle^{*T} &\approx \left[\left(\frac{d\sigma}{dx} \right)_e + \frac{1}{3ar_e} \left(\frac{d^2\sigma}{dx^2} \right)_e \right] (\langle x \rangle^T - \langle x \rangle^{*T}) + \dots \\ &\approx \left[\frac{d\sigma}{dr} \right]_e + \frac{1}{3a} \left(\frac{d^2\sigma}{dr^2} \right) (\langle \Delta r \rangle^T - \langle \Delta r \rangle^{*T}) \end{aligned} \quad (34)$$

and, when $\coth(hc\omega_e/2k_B T)$ is close to 1,

$$\begin{aligned} \langle \sigma \rangle^T - \langle \sigma \rangle^{*T} \approx & \left[\left(\frac{d\sigma}{dr} \right)_e + \frac{1}{3a} \left(\frac{d^2\sigma}{dr^2} \right)_e \right] \\ & \times \langle \Delta r \rangle_{\text{vib}}^T \left[1 - \left(\frac{\mu}{\mu^*} \right)^{1/2} \right] \end{aligned} \quad (35)$$

In equations (34) and (35), the first quantity (in square brackets) is a mass-independent purely electronic quantity; the second quantity is a mass-dependent dynamic factor. As we have seen, both the first and second derivatives of the shielding surface are most often negative. Right here, we see that the sign of the isotope shift is negative owing to $(d\sigma/dr)_e$ being negative, since the shift is defined such that the dynamic factor is positive; that is, the nucleus in the light isotopomer is less shielded (appears at higher frequency) than the nucleus in the heavy isotopomer. The unusual (positive) sign of the isotope shift will be observed when the shielding derivative is positive, such as for ^{23}Na in NaH or ^7Li in LiH . For polyatomic molecules, it makes physical sense to expand the nuclear shielding in terms of the normal coordinates Q_s (a concept of significance only for small displacements):^{21,37}

$$\sigma = \sigma_e + \sum_s \left(\frac{\partial \sigma}{\partial Q_s} \right)_e Q_s + \frac{1}{2} \sum_{s,r} \left(\frac{\partial^2 \sigma}{\partial Q_r \partial Q_s} \right)_e Q_r Q_s + \dots \quad (36)$$

where the shielding derivatives are taken at the equilibrium configuration. Normal coordinates are a logical choice for this expansion, since methods of evaluating the average values $\langle Q_s \rangle$ and $\langle Q_r Q_s \rangle$ are well known in vibrational spectroscopy. However, the derivatives of the nuclear shielding with respect to the mass-dependent normal coordinates are not invariant under isotopic substitution. For the purpose of discussing the isotope shift, it is more convenient to expand the shielding in terms of mass-independent internal displacement coordinates:^{5,21}

$$\sigma = \sigma_e + \sum_i \left(\frac{\partial \sigma}{\partial \mathcal{Y}_i} \right)_e \mathcal{Y}_i + \frac{1}{2} \sum_{ij} \left(\frac{\partial^2 \sigma}{\partial \mathcal{Y}_i \partial \mathcal{Y}_j} \right)_e \mathcal{Y}_i \mathcal{Y}_j + \dots \quad (37)$$

where \mathcal{Y}_i stands for the bond displacements (Δr_i) and the bond angle deformations ($\Delta \alpha_{ij}$).

The theoretical interpretation of isotope shifts in polyatomics therefore involves the mass-independent electronic quantities such as

$$\left(\frac{\partial \sigma}{\partial \mathcal{Y}_i} \right)_e = \left(\frac{\partial \sigma}{\partial \Delta r} \right)_e, \quad \left(\frac{\partial \sigma}{\partial \Delta \alpha} \right)_e, \quad \dots \quad (38)$$

which describe the change in nuclear shielding with bond extension or angle deformation, and the mass-dependent thermal averages $\langle \mathcal{Y}_i \rangle^T$, which are $\langle \Delta r \rangle^T$, $\langle \Delta \alpha \rangle^T$, ... and $\langle \mathcal{Y}_i \mathcal{Y}_j \rangle^T$, which are $\langle (\Delta r)^2 \rangle^T$, $\langle (\Delta \alpha)^2 \rangle^T$, $\langle \Delta r \Delta \alpha \rangle^T$, The isotope shift is given by

$$\begin{aligned} \sigma - \sigma^* = & \sum_i \left(\frac{\partial \sigma}{\partial \mathcal{Y}_i} \right)_e (\langle \mathcal{Y}_i \rangle^T - \langle \mathcal{Y}_i \rangle^{*T}) \\ & + \frac{1}{2} \sum_{ij} \left(\frac{\partial^2 \sigma}{\partial \mathcal{Y}_i \partial \mathcal{Y}_j} \right)_e (\langle \mathcal{Y}_i \mathcal{Y}_j \rangle^T - \langle \mathcal{Y}_i \mathcal{Y}_j \rangle^{*T}) + \dots \end{aligned} \quad (39)$$

In order to be able to evaluate $\langle \mathcal{Y}_i \rangle^T$, $\langle \mathcal{Y}_i \mathcal{Y}_j \rangle^T$ etc., we need a potential surface in which the vibrational motion of the molecule takes place. The known derivatives of this surface are the quadratic, cubic, etc. force constants. Normal coordinate analysis with the quadratic force constants gives the solutions to the harmonic problem, which are the harmonic frequencies ω_s , the normal coordinates Q_s , and the \mathbf{L} matrix. The internal displacement coordinates $\mathcal{Y} = \Delta r_j, \Delta \alpha_{ij}$, etc. can be expressed in terms of these normal coordinates in the general relation³⁸

$$\mathcal{Y} = \mathbf{Q} \quad (40)$$

where is a tensor containing the transformation coefficients between the curvilinear internal coordinates and various powers of Q_s . The vibrational part of Δr_i is then

$$\Delta r_i = \sum_i L_i^r Q_r + \frac{1}{2} \sum_{r,s} L_i^{rs} Q_r Q_s + \frac{1}{6} \sum_{r,s,t} L_i^{rst} Q_r Q_s Q_t + \dots \quad (41)$$

Thus, the vibrational average $\langle \Delta r \rangle_{\text{vib}}$ can be expressed in terms of $\langle Q_r \rangle$, $\langle Q_r Q_s \rangle$, etc. The analytical expressions for elements of the \mathbf{L} tensor are given by Hoy et al.,³⁸ in which the linear terms L_i^r are identical to the elements L_{ir} of the \mathbf{L} matrix. The above equation is exact, but in practice, of course, the series must be truncated; in general, it converges well, each term being smaller than the preceding by a factor of about 10 for typical vibrational amplitudes. The expectation values of only totally symmetric coordinates Q_s are required.³⁹

$$\langle Q_s \rangle = \left(\frac{h}{4\pi^2 c} \right)^{1/2} \omega_s^{-3/2} \left[3k_{sss} \left(\nu_s + \frac{1}{2} \right) + \sum_r k_{srr} \left(\nu_r + \frac{1}{2} g_r \right) \right] \quad (42)$$

where ω_s are the normal frequencies and k_{srr} are the cubic force constants, both in wavenumbers. g_r denotes the degeneracy of the r th vibration. $\langle Q_r Q_s \rangle = 0$ if $\omega_r \neq \omega_s$, and

$$\langle Q_s^2 \rangle = \frac{h}{4\pi^2 c \omega_s} \left(\nu_s + \frac{1}{2} \right) \quad (43)$$

To obtain the thermal average shielding, we again need $\langle \nu_s + \frac{1}{2} \rangle^T$. For larger molecules, it becomes impossible to calculate a sufficient number of rovibrational states in order to use the exact method for the thermal averaging, so the only practical way of calculating expectation values of molecular properties over different rotational and vibrational states for a given temperature is by using the harmonic approximation for the vibrational partition function, that is,

$$\left\langle \nu_s + \frac{1}{2} \right\rangle^T = \frac{1}{2} \coth(hc\omega_s/2k_B T) \quad (44)$$

3.4 Relative Magnitudes of Terms That Contribute to the Isotope Shift

Mass substitution at one site in the molecule affects dynamic averages of all electronic properties. If, in particular, we have nuclear spins at various sites, all of these will have different average shifts; some will experience larger changes than others. In general, the entire molecule participates in the dynamic averaging. Depending on the nature of each nuclear shielding surface, the change in chemical shift may be of either sign. Each molecule offers a unique situation, and, especially for the long-range isotope effects, vibrations involving many atoms may play a part. To illustrate the types of terms that contribute to a one-bond isotope shift, we use the

$^1\Delta$ ^{13}C ($^2/1\text{H}$) in CH_4 as an example. During vibration, the displacements away from the equilibrium nuclear configuration can be small enough that a Taylor series expansion can be used:⁴⁰

$$\begin{aligned} \langle \sigma^{\text{C}} \rangle = & \sigma_{\text{e}} + P_r(\langle \Delta r_1 \rangle + \langle \Delta r_2 \rangle + \langle \Delta r_3 \rangle + \langle \Delta r_4 \rangle) \\ & + \frac{1}{2} P_{rr}[\langle (\Delta r_1)^2 \rangle + \langle (\Delta r_2)^2 \rangle + \langle (\Delta r_3)^2 \rangle + \langle (\Delta r_4)^2 \rangle] \\ & + P_{rs}(\langle \Delta r_1 \Delta r_2 \rangle + \langle \Delta r_1 \Delta r_3 \rangle + \langle \Delta r_1 \Delta r_4 \rangle \\ & + \langle \Delta r_2 \Delta r_3 \rangle + \langle \Delta r_2 \Delta r_4 \rangle + \langle \Delta r_3 \Delta r_4 \rangle) \\ & + \frac{1}{2} P_{\alpha\alpha}[\langle (\Delta \alpha_{12})^2 \rangle + \dots] + P_{\alpha\beta}(\langle \Delta \alpha_{12} \Delta \alpha_{13} \rangle + \dots) \\ & + P_{r\alpha}(\langle r_1 \Delta \alpha_{12} \rangle + \dots) + P_{\alpha\omega}(\langle \Delta \alpha_{12} \Delta \alpha_{34} \rangle + \dots) \\ & + \text{higher-order terms} \end{aligned} \quad (45)$$

where $P_r \equiv (\partial \sigma^{\text{C}} / \partial r_1)_{\text{e}}$, while P_{rr} and P_{rs} are the second derivatives of the ^{13}C shielding with respect to the C–H bond distances; $P_{\alpha\alpha}$, $P_{\alpha\beta}$, and $P_{\alpha\omega}$ are the second derivatives of the ^{13}C shielding with respect to the HCH bond angles, and $P_{r\alpha}$ is the mixed second derivative $(\partial^2 \sigma^{\text{C}} / \partial r_1 \partial \alpha_{12})_{\text{e}}$. In some molecules, there are first derivatives with respect to the angle as well, for example, for ^{17}O in H_2O and ^{31}P in PH_3 .^{41,42} In yet others, the averaging cannot be carried out by considering small displacements, as in the inversion motion of the NH_3 molecule. The complexity of the equation increases with increasing number of atoms. Nevertheless, many general trends may be observed in the huge body of information represented in tables of thousands of isotope shifts.^{1–3} These trends have become apparent, despite the uniqueness of the dynamic averaging of each molecule, because some terms in the full theory are more dominant than others. It is the persistence of the dominant contributions in most molecules that allows us to consider isotope shifts in much simpler terms, short of full averaging of full shielding surfaces in every case. In Table 7, we examine the relative magnitudes of terms that contribute to the isotope shift in selected molecules, where the calculations of the many terms (as shown above for CH_4) have been carried out to gain some insight into what might be expected in other molecules.^{36,42–46} Clearly, the mixed terms and higher-order terms (listed in Table 7 as ‘Other’) are negligible compared with the total isotope shift. The P_r term, which is due entirely to the anharmonicity of the vibration, provides the largest contribution, but P_{rr} terms are not negligible. The stretch (P_r and P_{rr} terms together) dominate, even in the case of NH_3 , where the inversion mode gives significant angle deformation contributions. If we can extrapolate these results to larger molecules, we can say that the bond stretching contributions dominate one-bond isotope shifts, and the anharmonic part of this, which goes with the first

Table 8 Comparison of Shielding Derivatives Estimated from Isotope Shifts with Those Obtained from Ab Initio Quantum Mechanical Calculations

	$(\partial \sigma / \partial r)_e$ (ppm \AA^{-1})	
	Estimated from isotope shifts	Ab initio theoretical
^{15}N in CN^-	–872 ⁴⁷	–809.8 ³⁴
^{13}C in CN^-	–473 ⁴⁷	–494.4 ³⁴
^{15}N in NH_3	–124 ¹⁷	–123.2 ³⁶
^{15}N in NH_4^+	–65 ²⁷	–67.9 ⁵²
^{31}P in PH_3	–180 ¹⁵	–148.83 ⁴²
^{13}C in CH_4	–38 ⁴⁸	–52.62 ⁵³
^{17}O in H_2O	–294 ¹⁷	–270.9 ⁴¹
^{77}Se in H_2Se	–1250 ⁴⁹	–1056.5 ⁴⁶
^{13}C in CO	–456 ¹²	–538.1 ³⁴
^{17}O in CO	–1150 ¹²	–1061.1 ³⁴
^{15}N in N_2	–912 ⁵⁰	–1011.4 ³⁴
^{11}B in BH_4^-	–26.7 ²⁷	–27.0 ⁵²
^{13}C in CO_2	–214 ⁵¹	–156.4 ³⁴
^{15}N in NO_2^-	–990 ⁵¹	–1438.1 ³⁴
^{15}N in NO_3^-	–410 ⁵¹	–498.0 ³⁴

shielding derivative $(\partial \sigma / \partial r)_e$, gives the largest contribution. However, the terms involving the second derivative $(\partial^2 \sigma / \partial r^2)_e$ are also important. Bond angle contributions are uniformly less important than the bond stretching contributions to the isotope shift.

If we take the experimental isotope shift and use an estimate for the dynamic factor $\langle \Delta r_{\text{XH}} \rangle - \langle \Delta r_{\text{XD}} \rangle$, we arrive at a reasonable estimate of the shielding derivative $(\partial \sigma / \partial r)_e$ in the molecule. Indeed, Table 8 shows that the estimated shielding derivatives compare reasonably well with the derivatives obtained from the ab initio shielding surfaces.

3.5 Additivity of Isotope Shifts

We can use the isotopomers of the CH_4 molecule to illustrate the additivity of NMR isotope shifts. The mean bond displacements in the methane family $\text{CX}_{4-n}\text{Y}_n$ (where X, Y = H, D, T) have been calculated using the anharmonic force field of methane.¹⁹ It has been found that the substitution effects on the vibrational contribution to mean bond displacements are strictly additive. Each substitution of a hydrogen by a deuterium shortens the appropriate bond by nearly the same amount Δ . The mean bond displacements in $^{12}\text{CH}_{4-n}\text{T}_n$ and $^{12}\text{CD}_{4-n}\text{T}_n$ exhibit the same strictly linear dependence on n . We can express $\langle \Delta r_{\text{CH}} \rangle$ and $\langle \Delta r_{\text{CD}} \rangle$ in $^{12}\text{CH}_{4-n}\text{D}_n$ as follows. If we let

$$d = \langle \Delta r_{\text{CH}} \rangle \quad \text{in } \text{CH}_4 \text{ at } 300 \text{ K} \quad (46)$$

Table 7 Isotope Shifts $\sigma^{\text{X}}(\text{XH}_n) - \sigma^{\text{X}}(\text{XD}_n)$ (in ppm) Calculated for ^{13}C , ^{15}N , ^{31}P , ^{17}O , and ^{77}Se Nuclei

Term	CH_4 ⁴³	NH_3 ³⁶	PH_3 ⁴²	H_2O ⁴⁴	H_2Se ^a
P_r	–1.169	–2.05	–2.44	–2.847	–11.66
P_{rr}	0.453	–0.97	–1.68	–1.316	–5.59
$P_{\alpha} + P_{\alpha\alpha}$	+0.686	+0.66	+0.67	+0.404	+1.25
Other	–0.042	–0.004	0.002	+0.08	neglect
Total	–0.978	–2.36	–3.45	–3.68	–16.0
Experimental	–0.774	–1.87	–2.53	–3.09	–14.04

^aCalculated by Jameson,⁴⁵ based on the points on the ab initio shielding surface of Tossell and Lazzarotti.⁴⁶

$$d - \Delta = \langle \Delta r_{\text{CD}} \rangle \quad \text{in } \text{CD}_4 \text{ at } 300 \text{ K} \quad (47)$$

where $d = 2.0881 \text{ pm}$ and $\Delta = 0.553 \text{ pm}$, we find for $\text{CH}_{4-n}\text{D}_n$ that

$$\langle \Delta r_{\text{CD}} \rangle = d - \Delta + (4 - n)\delta_{\text{D}} \quad (48)$$

$$\langle \Delta r_{\text{CH}} \rangle = d + n\delta_{\text{H}} \quad (49)$$

Similar relations can be found for the other series of isotopomers. That is, for a given bond, substitution of an isotope involved in this bond had an effect Δ on its own mean bond length (a primary effect on the mean bond displacement); each substitution of an isotope at some other bond has a much smaller effect δ (a secondary effect). The $^2/1\text{H}$ -induced ^{13}C NMR isotope shift between any two isotopomers of $\text{CH}_{4-n}\text{D}_n$ can then be expressed as

$$\begin{aligned} \sigma^{\text{C}}(\text{CH}_{4-n}\text{D}_n) - \sigma^{\text{C}}(\text{CH}_{4-n'}\text{D}_{n'}) &= \left(\frac{\partial \sigma^{\text{C}}}{\partial r} \right)_e \\ &\quad \times [(n' - n)\Delta + \text{terms in } \delta] \\ &\approx \left(\frac{\partial \sigma^{\text{C}}}{\partial r} \right)_e (n' - n)\Delta \quad (50) \end{aligned}$$

This is the basis for the near-additivity of isotope shifts due to substitution at equivalent sites. If we leave out the terms in δ (which are about two orders of magnitude smaller than Δ), we have strict additivity: the magnitude of the shift is proportional to the number $n' - n$ of atoms that have been substituted by isotopes. Even when all the terms in P_{rr} , P_{rs} , P_{rs} , etc. are included and calculated properly, the nearly strict additivity of isotope shifts is preserved. Although there are many smaller changes that are not quite the same as each ^mX is replaced by $^{m'}\text{X}$, it has been shown that these smaller changes lead to only slight deviations from additivity, which deviations incidentally have been observed^{15–18} just as predicted.¹⁹

4 GENERAL TRENDS IN THE ELECTRONIC FACTORS

We have already seen that the dynamical factors in one-bond isotope shifts are fairly predictable, and can even be estimated without a good force field because the mass-independent part of the dynamic factor is largely determined by the bond length and the rows of the Periodic Table of the pair of bonded atoms. We have also seen that the mass dependence of the isotope shift and its additivity can be explained entirely by the dynamic factors for one-bond isotope shifts. All other trends must therefore be attributable to trends in the electronic factor and the first and second derivatives of the nuclear shielding. If we estimate the dynamic factors $\langle \Delta r \rangle - \langle \Delta r \rangle^*$ as described in Section 3.1, it is possible to obtain the magnitudes and signs of the electronic factor $[(\partial\sigma/\partial r)_e + (1/3a)(\partial^2\sigma/\partial r^2)_e]$, which we shall denote simply by $(\partial\sigma/\partial r)_e$, with the understanding that the first-derivative terms nearly always dominate, although the ratio of the above two terms may range from 10:1 to 3:1.

Some trends in $(\partial\sigma/\partial r)_e$ have been predicted from the observed trends in isotope shifts.^{5,6} Recent ab initio calculations have explored the generality of these trends and the limits and conditions of their applicability.³⁴

- $(\partial\sigma/\partial r)_e$ is usually negative. The general shape of the shielding surface shown in Figure 4 seems to be typical for a diatomic molecule, and, for most nuclei, the minimum in the shielding surface occurs at separations larger than the equilibrium internuclear separation, leading to a negative $(\partial\sigma/\partial r)_e$. The exceptional sign of $(\partial\sigma/\partial r)_e$ arises when the minimum in the shielding surface lies inside the equilibrium internuclear separation, as in Figure 5. In polyatomic molecules, negative $(\partial\sigma/\partial r)_e$ are also much more commonly found than positive ones, leading to the usual (negative) sign of the isotope shift.
- $(\partial\sigma/\partial r)_e$ generally increases with the chemical shift range of the nucleus. We have seen in Figure 6 that changes in the shielding upon displacement away from the equilibrium geometry do scale in analogous compounds according to $\langle a_0^3/r^3 \rangle$ for the free atom, which is the same factor that varies periodically across the Periodic Table in the same way as the ranges of chemical shifts.^{54,55} Because of this correlation, an easy way to obtain an estimate of an isotope shift is to use the scaling factor of $\langle a_0^3/r^3 \rangle$ values to provide a Periodic-Table-wide set of 'reduced isotope shifts', which need only be multiplied by the mass factors $[(m' - m)/m'] \times (m_A + m)/2m_A$ to get an estimate of the one-bond isotope shift induced by any isotopic substitution for any nucleus in any molecule.⁵⁶
- $(\partial\sigma/\partial r)_e$ has been found to correlate with the absolute shielding σ_0 in related molecules: at the equilibrium geometry, the most deshielded environments have more steeply changing shielding surfaces. When the dynamic terms are very similar, this forms the basis for the correlations of $^1\Delta$ with chemical shifts, which have been observed in some cases. Such correlations of isotope shifts are more likely to be noticed in diatomic-like situations such as $^{13/12}\text{C}$ -induced ^{19}F isotope shifts or $^{18/16}\text{O}$ -induced ^{13}C isotope shifts in $\text{O}=\text{C}$ situations.⁵⁷ Chesnut and Wright have found that calculated shielding derivatives do roughly correlate with shielding itself for ^{19}F and for ^{13}C , ^{15}N , and ^{17}O involved in multiple bonds.
- The magnitudes of the derivatives of shielding with respect to extension of a bond increase with increasing bond order. Since bond lengths tend to anticorrelate with bond order (higher bond order, shorter bond length), this trend in the shielding derivative is also the basis for the observed increasing magnitudes of one-bond isotope shifts for shorter bond lengths between the NMR nucleus and the substitution site.
- The shielding derivative tends to be more negative with increasing negative net charge and with the presence of lone pairs on the observed nucleus. This has been found in the comparisons of ^{15}N in NO_2^- and NO_3^- , ^{15}N in NH_3 and NH_4^+ , ^{31}P in PH_4^+ , PH_3 and PH_2^- , ^{119}Sn in SnH_3^+ , SnH_4 and SnH_3^- , and ^{13}C and also ^{15}N in HCN and CN^- .
- Since the one-bond coupling constant is a purely electronic quantity, it must be the electronic factors in the one-bond isotope shifts that allow the observation of linear correlations with the one-bond coupling constant, and likewise the incremental effects of substitution of H by Ph or H by CH_3 in the examples in Table 9.^{10–61} These above data translate to increasingly negative $(\partial\sigma^{\text{X}}/\partial r_{\text{XH}})_e$ upon successive Ph substitution at X.

Table 9

	$^1\Delta$ (ppm per D)		$^1\Delta^{13}\text{C}(^{2/1}\text{H})$ (ppm per D)
^{15}N in NH_3	-0.623	^{13}C in CH_3D	-0.187
in PhNH_2	-0.715	in PhCH_2D	-0.2755
^{31}P in PH_3	-0.846	in $(\text{Ph})_2\text{CHD}$	-0.342
in PhPH_2	-1.21	in $(\text{Ph})_3\text{CD}$	-0.4377
^{13}C in CH_4	-0.192	^{13}C in CH_3D	-0.187
in PhCH_3	-0.28	in $\text{H}_3\text{CCH}_2\text{D}$	-0.284
^{77}Se in SeH_2	-7.02	in $(\text{H}_3\text{C})_2\text{CHD}$	-0.3759
in PhSeH	-7.96	in $(\text{H}_3\text{C})_3\text{CD}$	-0.4722

5 ISOTOPE SHIFTS OVER TWO OR MORE BONDS

Isotope shifts due to substitution with a heavier atom at a site remote from the observed nucleus show the same general trends as one-bond isotope shifts.

1. The sign is still generally negative, although some are positive, with some alternation of signs being observed in the same molecule.
2. The magnitude reflects the chemical shift range of the observed nucleus.
3. The magnitude is related to the fractional mass change.
4. The effect is additive.

These are generally smaller than one-bond shifts; nevertheless, a large number of them have been observed, some over a distance of seven or more bonds. The question is, what information is contained in these long-range shifts? What we propose to show here is that these long-range shifts are a property of the electronic transmission path from the site of substitution up to the resonant nucleus.

To illustrate the types of terms that contribute to a long-range isotope shift, let us consider a two-bond isotope shift such as $^2\Delta^{13}\text{C}(^{2/1}\text{H})$ in CH_4 .¹⁹ The average proton shielding for proton H_1 can be written as

$$\begin{aligned}
 \langle\sigma^{\text{H}_1}\rangle &= \sigma_e + P_r\langle\Delta r_1\rangle + P_s(\langle\Delta r_2\rangle + \langle\Delta r_3\rangle + \langle\Delta r_4\rangle) \\
 &+ \frac{1}{2}P_{rr}(\langle\Delta r_1\rangle^2) + \frac{1}{2}P_{ss}[(\langle\Delta r_2\rangle^2) + (\langle\Delta r_3\rangle^2) + (\langle\Delta r_4\rangle^2)] \\
 &+ P_{rs}(\langle\Delta r_1\Delta r_2\rangle + \langle\Delta r_1\Delta r_3\rangle + \langle\Delta r_1\Delta r_4\rangle) \\
 &+ P_{st}(\langle\Delta r_2\Delta r_3\rangle + \langle\Delta r_2\Delta r_4\rangle + \langle\Delta r_3\Delta r_4\rangle) + \dots
 \end{aligned}
 \quad (51)$$

where

$$P_r \equiv \left(\frac{\partial\sigma^{\text{H}_1}}{\partial r_1}\right)_e, \quad P_s \equiv \left(\frac{\partial\sigma^{\text{H}_1}}{\partial r_2}\right)_e \quad (52)$$

and P_{rr} , P_{ss} , P_{rs} , and P_{st} are the appropriate second derivatives of the shielding with respect to the various C–H distances. Therefore, the two-bond deuterium-induced proton isotope shifts between CH_3D and CH_4 is (with D replacing proton number 2)

$$\begin{aligned}
 ^2\Delta^{13}\text{C}(^{2/1}\text{H}) &= \langle\sigma^{\text{H}_1}\rangle_{\text{CH}_4} - \langle\sigma^{\text{H}_1}\rangle_{\text{CH}_3\text{D}} \\
 &= (P_r + 2P_s)(\langle\Delta r_1\rangle_{\text{CH}_4} - \langle\Delta r_1\rangle_{\text{CH}_3\text{D}}) \\
 &+ P_s(\langle\Delta r_2\rangle_{\text{CH}_4} - \langle\Delta r_2\rangle_{\text{CH}_3\text{D}}) \\
 &+ (\frac{1}{2}P_{rr} + P_{ss})[(\langle\Delta r_1\rangle^2)_{\text{CH}_4} - (\langle\Delta r_1\rangle^2)_{\text{CH}_3\text{D}}] \\
 &+ \frac{1}{2}P_{ss}[(\langle\Delta r_2\rangle^2)_{\text{CH}_4} - (\langle\Delta r_2\rangle^2)_{\text{CH}_3\text{D}}] \\
 &+ (P_{rs} + 2P_{st})(\langle\Delta r_1\Delta r_2\rangle_{\text{CH}_4} - \langle\Delta r_1\Delta r_2\rangle_{\text{CH}_3\text{D}}) \\
 &+ (2P_{rs} + P_{st})(\langle\Delta r_1\Delta r_3\rangle_{\text{CH}_4} - \langle\Delta r_1\Delta r_3\rangle_{\text{CH}_3\text{D}})
 \end{aligned}
 \quad (53)$$

With D replacing proton number 2, $\delta = \langle\Delta r_i\rangle_{\text{CH}_4} - \langle\Delta r_i\rangle_{\text{CH}_3\text{D}}$ is (the same for $i = 1, 3, 4$) a slight change of about 10^{-3} pm in the other C–H average bond lengths due to deuteration, and $\langle\Delta r_2\rangle_{\text{CH}_4} - \langle\Delta r_2\rangle_{\text{CH}_3\text{D}}$ is the typical $\Delta = \langle r_{\text{CH}}\rangle - \langle\Delta r_{\text{CD}}\rangle$, which is of order about 0.5 pm:

$$\begin{aligned}
 ^2\Delta^{13}\text{C}(^{2/1}\text{H}) &\approx (P_r + 2P_s)\delta + P_s\Delta + (\frac{1}{2}P_{rr} + P_{ss})\delta_{rr} + \frac{1}{2}P_{ss}\Delta_{rr} \\
 &+ (P_{rs} + 2P_{st})\Delta_{rs} + (2P_{rs} + P_{st})\delta_{rs}
 \end{aligned}
 \quad (54)$$

If we invoke the relationship $\langle\Delta r\rangle \approx \frac{3}{2}ar_e \langle(\Delta r)^2\rangle$ used earlier, we find

$$\begin{aligned}
 ^2\Delta^{13}\text{C}(^{2/1}\text{H}) &\approx \left(P_s + \frac{1}{3a}P_{ss}\right)\Delta + \left(P_r + \frac{1}{3a}P_{rr} + 2P_s + \frac{2}{3a}P_{ss}\right)\delta \\
 &+ \text{mixed terms} + \text{higher-order terms}
 \end{aligned}
 \quad (55)$$

or, more succinctly,

$$\begin{aligned}
 2\Delta^{13}\text{C}(^{2/1}\text{H}) &\approx \mathcal{S}\Delta + (\mathcal{P} + 2\mathcal{S})\delta \\
 &+ \text{mixed terms} + \text{higher-order terms}
 \end{aligned}
 \quad (56)$$

Here \mathcal{P} stands for the following combination of primary first and second derivatives:

$$\mathcal{P} \equiv \left(\frac{\partial\sigma^{\text{H}_1}}{\partial r_1}\right)_e + \frac{1}{3a}\left(\frac{\partial^2\sigma^{\text{H}_1}}{\partial r_1^2}\right)_e \quad (57)$$

and is a measure of the sensitivity of the shielding of a nucleus to stretching of a bond to it. \mathcal{S} stands for the following combination of secondary first and second derivatives:

$$\mathcal{S} \equiv \left(\frac{\partial\sigma^{\text{H}_1}}{\partial r_2}\right)_e + \frac{1}{3a}\left(\frac{\partial^2\sigma^{\text{H}_1}}{\partial r_2^2}\right)_e \quad (58)$$

and is a measure of the sensitivity of the shielding of a nucleus to stretching of a remote bond.¹⁹ When we recall that $\Delta \approx 0.5$ pm whereas $\delta \approx 10^{-3}$ pm, we see that the term $\mathcal{S}\Delta$ would dominate the isotope shift unless \mathcal{P} is two orders of magnitude larger than \mathcal{S} . It is therefore valid to consider a long-range isotope shift as largely described by a product of a primary change in the average bond length at the heavy atom substitution site (the dynamic factor) and a secondary shielding derivative(s) that measures the change in shielding upon a change with bond length at the remote site. This is very encouraging, because the secondary dynamic factor δ is so dependent on the entire molecular framework and potential energy surface in which vibrations take place that it is difficult to estimate. On the other hand, we have seen that Δ has a very straightforward dependence on r_e and the masses in the local fragment, and can be easily estimated. This means that if the δ terms are unimportant, the sign and magnitude of the long-range isotope shifts are a direct measure of the sign and

magnitude of $(\partial\sigma/\partial r_{\text{remote}})_e$. This derivative is stereospecific, dependent on electron-withdrawing/donating abilities of substituents, and has the usual electronic-transmission-path dependence of various observables such as long-range spin-spin coupling and substituent effects on chemical shifts. Thus, in $^{13}\text{CH}_3(\text{CH}_2)_{n-2}\text{NHD}$, for example,

$${}^n\Delta^{13}\text{C}^{(2/1)\text{H}} \approx \left[\left(\frac{\partial\sigma^{\text{C}}}{\partial r_{\text{NH}}} \right)_e + \frac{1}{3a} \left(\frac{\partial^2\sigma^{\text{C}}}{\partial r_{\text{NH}}^2} \right)_e \right] \times (\langle\Delta r_{\text{NH}}\rangle - \langle\Delta r_{\text{ND}}\rangle) \quad (59)$$

it is easy to see why n -bond isotope shifts are in general smaller than one-bond isotope shifts. The farther away the substitution site is from the observed nucleus, the smaller the secondary derivative is expected to be. For example, in the H_2O molecule,⁴¹

$$\begin{aligned} \left(\frac{\partial\sigma^{\text{H}_1}}{\partial r_{\text{OH}_1}} \right)_e &= -0.353 \text{ ppm pm}^{-1} \\ \left(\frac{\partial\sigma^{\text{H}_1}}{\partial r_{\text{OH}_2}} \right)_e &= -0.046 \text{ ppm pm}^{-1} \end{aligned} \quad (60)$$

that is, a trace along the increasing coordinate r_{OH_1} gives a sharply decreasing H_1 shielding surface near the equilibrium geometry, but a trace along the coordinate r_{OH_2} on the same shielding surface is rather flat. Also, the nearly flat portion of the shielding surface could be sloping slightly in either direction; thus, either sign is possible for long-range isotope shifts. The secondary derivatives should still reflect the shielding sensitivity of various nuclei as manifested in the ranges of their chemical shifts.

The experimental evidence for the dominance of the term $S\Delta$ is convincing.

1. The observed additivity of long-range isotope shifts is completely consistent with this. Isotope shifts from equivalent substitution sites such as a remote CH_3 group involve the secondary derivative multiplied by one Δ term for each C–D replacing a C–H.
2. The mass dependence of the two-bond isotope shift is the same as that of the one-bond shift, that is, $1-(\mu/\mu^*)^{1/2}$, where μ and μ^* are the local reduced masses at the substitution site. Furthermore, the ratio of the effects of substitution of H by T to that of H by D is the same as would be expected if the Δ term dominated the isotope shift. Vibrational calculations show that⁴⁸

$$\frac{\langle\Delta r_{\text{CH}}\rangle_{\text{CH}_4} - \langle\Delta r_{\text{CT}}\rangle_{\text{CT}_4}}{\langle\Delta r_{\text{CH}}\rangle_{\text{CH}_4} - \langle\Delta r_{\text{CD}}\rangle_{\text{CD}_4}} = 1.426 \quad (61)$$

In $(\text{CH}_3)_2\text{C}=\text{O}$, the observed ratio of isotope shifts for tritium and deuterium substitution is¹¹

$$\frac{{}^1\Delta^{13}\text{C}^{(3/1)\text{H}}}{{}^1\Delta^{13}\text{C}^{(2/1)\text{H}}} = 1.424 \pm 0.025 \quad (62)$$

That this ratio is indistinguishable from 1.426 serves to reassure us that the leading term is dominant in one-bond shifts, with $(\partial\sigma/\partial r)_e (\langle\Delta r_{\text{CH}}\rangle - \langle\Delta r_{\text{CD}}\rangle)$ for deuterium substitution and $(\partial\sigma/\partial r)_e (\langle\Delta r_{\text{CH}}\rangle - \langle\Delta r_{\text{CT}}\rangle)$ for tritium substitution. The two-bond isotope shifts have also been observed in $\text{CH}_3^{13}\text{C}(\text{O})\text{CH}_3$, and these have the ratio¹¹

$$\frac{{}^2\Delta^{13}\text{C}^{(3/1)\text{H}}}{{}^2\Delta^{13}\text{C}^{(2/1)\text{H}}} = 1.41 \quad 0.12 \quad (63)$$

This ratio is also indistinguishable from 1.426, which indicates that the dominant contribution is $(\partial\sigma^{\text{C}(\text{O})}/\partial r_{\text{CH}})_e \times (\langle\Delta r_{\text{CH}}\rangle - \langle\Delta r_{\text{CT}}\rangle)$ for tritium substitution and $(\partial\sigma^{\text{C}(\text{O})}/\partial r_{\text{CH}})_e (\langle\Delta r_{\text{CH}}\rangle - \langle\Delta r_{\text{CD}}\rangle)$ for deuterium substitution.

3. The relative signs of one-bond and n -bond isotope shifts for the same nucleus in the same molecule are not always the same. Consider, for example, the carbonyl carbon isotope shifts in $(\text{CH}_3)_2^{13}\text{C}=\text{O}$. The ${}^1\Delta^{13}\text{C}^{(18/16)\text{O}}$ and ${}^2\Delta^{13}\text{C}^{(2/1)\text{H}}$ are opposite signs. Thus, the important term in ${}^2\Delta^{13}\text{C}^{(2/1)\text{H}}$ must not involve $(\partial\sigma^{\text{C}(\text{O})}/\partial r_{\text{CO}})_e \delta$.
4. The long-range isotope shifts correlate with indicators of electronic transmission paths such as dihedral angle dependence of three-bond isotope shifts (similar to the Karplus relation for three-bond coupling constants, although not with one set of coefficients), stereospecificity (*cis* versus *trans* versus *gauche*, and *syn* versus *anti*) of isotope shifts parallels that of spin-spin coupling, and the correlation of long-range isotope shifts with electron-withdrawing/donating ability of substituents, even across a path traversing seven bonds. These correlations of long-range isotope shifts with purely electronic quantities can only be observed if the isotope shift is itself dominated by an electronic factor that depends on the transmission of electronic information between the observed nucleus and the mass-modified site: a fortunate occurrence, since the long-range electronic factor is far more interesting and useful than the long-range dynamic factor. Since the primary dynamic factor Δ is easily estimated, long-range isotope shifts can provide direct invaluable information about the changes in shielding of a nucleus upon a minor perturbation at a distant site.

In summary, the electronic factor $(\partial\sigma^{\text{A}}/\partial r_{\text{XY}})_e$ in the long-range isotope shifts is found to have the following attributes.

1. The magnitude decreases (usually) as the Y–X bond becomes more remote from nucleus A. Ab initio calculations have shown that for the first- and second-row hydrides XH_n , the ratio $(\partial\sigma^{\text{H}_1}/\partial r_2)_e/(\partial\sigma^{\text{H}_1}/\partial r_1)_e = 0.06\text{--}0.14$. However, the two-bond secondary derivative is not necessarily much smaller than primary derivatives, especially when multiple bonds are involved.³⁴
2. It is stereospecific. For three-bond isotope shifts, it is found that *cis*, *trans* > *gauche*, and in some cases the dihedral angle dependence has been clearly observed and it is not unlike the Karplus relation of three-bond spin-spin coupling with angle ϕ . This stereospecificity is purely electronic in nature.
3. It correlates with other purely electronic quantities that are dependent on the same electronic transmission path, such as substituent effects on chemical shifts by electron-withdrawing or -donating groups. The electronic transmission path is most easily explored by the isotope shift, because substitution of an atom by a heavier one leads to the fewest complications compared with other methods of investigation such as replacement by atoms or groups of different electronegativity or size.

6 ISOTOPE EFFECTS ON SPIN-SPIN COUPLING

The indirect spin-spin coupling constant J is a useful index of the chemical bond, and isotope effects on it provide

information about the sensitivity of J to bond extension. Since the isotope effects on the isotropic average J can be determined more precisely than the individual J tensor components or the anisotropy, the isotope effects can be considered as *the* major source of experimental information for assessing the quality of ab initio theoretical calculations of indirect spin–spin coupling.

The working definitions of the isotope effects on J are as follows.⁴ $\Delta_s {}^n J(\text{AB})[{}^{m'}/{}^m\text{X}]$ is the *secondary* isotope effect on the n -bond coupling constant between nuclei A and B due to the substitution of ${}^m\text{X}$ by the heavier isotope ${}^{m'}\text{X}$ somewhere in the molecule:

$$\Delta_s {}^n J(\text{AB})[{}^{m'}/{}^m\text{X}] = |{}^n J(\text{AB})|^* - |{}^n J(\text{AB})| \quad (64)$$

$\Delta_p {}^n J(\text{A}^{2/1}\text{H})$ is the *primary* isotope effect on the coupling constant between nuclei A and H due to the substitution of H by D , the coupled nuclei being separated by n bonds:

$$\Delta_p {}^n J(\text{A}^{2/1}\text{H}) = |{}^n J(\text{AD})|^* \frac{\gamma_{\text{H}}}{\gamma_{\text{D}}} - |{}^n J(\text{AH})| \quad (65)$$

where $\gamma_{\text{H}}/\gamma_{\text{D}} = 6.514\,398\,04(120)$. Of course, if we instead use the purely electronic quantities, namely, the reduced coupling constants

$${}^n K(\text{AH}) \equiv 4\pi^2 \frac{{}^n J(\text{AH})}{h\gamma_{\text{A}}\gamma_{\text{H}}} \quad (66)$$

usually expressed in reduced units of $10^{19} \text{J}^{-1} \text{T}^2$, then the primary isotope effect is simply a difference:

$$\Delta_p {}^n K(\text{A}^{2/1}\text{H}) = |{}^n K(\text{AD})|^* - |{}^n K(\text{AH})| \quad (67)$$

Only the absolute values are compared, for practical reasons, since the absolute signs of spin–spin coupling constants are not always known. As in isotope shifts, the asterisk $*$ denotes the heavier isotopomer. Where both secondary and primary isotope effects are observed, the primary isotope effect should be obtained from, for example, $J(\text{SnD})$ in SnH_2D^- and $J(\text{SnH})$ in SnH_3^- , rather than $J(\text{SnD})$ and $J(\text{SnH})$ in the same isotopomer SnH_2D^- . The latter difference includes both primary and secondary isotope effects.

Isotope effects on nuclear shielding are usually visually obvious in a high-resolution NMR spectrum, since the peaks of the isotopomer are shifted from the parent species. On the other hand, isotope effects on coupling constants are only observed as very slightly different multiplet splittings for each isotopomer (secondary isotope effects) or as a slightly smaller (usually) or larger $J(\text{AD})$ than that expected from $J(\text{AH})/6.514\,398\,04$ (primary isotope effects). Because of this factor of 6.514..., the isotope effects on J are less precisely determined than the isotope effects on shielding. According to these working definitions, a positive isotope effect on J means that the reduced coupling is larger in the deuterated species.

6.1 Observed General Trends in Isotope Effects on J

The general trends and their theoretical explanation have been presented by Jameson and Osten.⁴

1. The sign of the primary or secondary isotope effect on the coupling constant is not directly related to the absolute sign of the coupling constant. Whether it is related to the absolute sign of the reduced coupling constant is not yet established, since one-bond coupling isotope effects are presently available for positive reduced coupling constants only.
2. Primary isotope effects are negative or positive, the positive signs being found only in molecules involving one or more lone pairs of the coupled nuclei. For example, primary isotope effects are positive in H_2Se , in PH_3 , and in other 3-coordinate phosphorus, but negative in PH_4^+ and in 4- and 5-coordinate phosphorus. It is positive in SnH_3^- (one lone pair) and negative in SnH_4 and SnH_3^+ (no lone pairs).
3. Secondary isotope effects can have either sign, but are often negative. Positive signs have been observed where triple bonds are involved (as in $\text{HC}\equiv\text{CH}$ and $\text{HC}\equiv\text{N}$), but also in some of the same systems with positive primary isotope effects.
4. Secondary isotope effects are roughly additive upon substitution of several equivalent sites neighboring the coupled nuclei. For example, in the NH_4^+ ion, each D substitution decreases ${}^1J(^{14}\text{NH})$ by 0.05 ± 0.02 Hz, and in PH_3 , each D substitution decreases ${}^1J(\text{PH})$ by 2.5 Hz. Small deviations from additivity have been observed.
5. The magnitudes of isotope effects are small, the largest primary effect being about 10% of the coupling constant in SnH_3^- , so that only the effects of deuterium (and tritium) substitution, where the largest fractional changes in mass are involved, have been observed. Some of the larger primary isotope effects are +11.5 Hz for $\Delta_p {}^1J(\text{PH})$ in PH_3 and +10.5 Hz in SnH_3^- . Secondary isotope effects as large as -2.0 Hz per D [for ${}^1J(\text{SiF})$] and +3.0 Hz per D [for ${}^1J(\text{SnH})$] have been observed.
6. The magnitudes of the isotope effects are roughly proportional to the fractional change in mass, in the very few instances where effects of isotopic substitution of ${}^1\text{H}$ by ${}^2\text{H}$ and ${}^3\text{H}$ have been reported.

6.2 Rovibrational Averaging of J , the Leading Terms

Just as in isotope shifts, the isotope effect on J can be written in terms of products of electronic and dynamic factors as follows.⁶ For a diatomic molecule,

$$\begin{aligned} \langle J \rangle^* - \langle J \rangle &= \left(\frac{\partial J}{\partial r} \right)_e (\langle \Delta r \rangle^* - \langle \Delta r \rangle) \\ &+ \frac{1}{2} \left(\frac{\partial^2 J}{\partial r^2} \right)_e [(\langle \Delta r \rangle^*)^2 - \langle \Delta r \rangle^2] + \dots \quad (68) \end{aligned}$$

The dynamic factors are the same as we have already discussed (and, indeed, the same for all rovibrational averaging of any molecular electronic properties). Only the electronic factors need be discussed here. Of course, γ of some nuclei are negative, so we really should compare derivatives of the reduced coupling such as $(\partial K/\partial r)_e$, etc., where

$$\left(\frac{\partial J}{\partial r} \right)_e = \frac{h\gamma_{\text{N}}\gamma_{\text{N}'}}{4\pi^2} \left(\frac{\partial K}{\partial r} \right)_e \quad (69)$$

One important difference between J and σ is that the latter is a one-center property whereas the former is a two-center

Table 10

	Experimental ¹⁵		Calculated	
	$K(\text{SnH})$ (reduced units)	$K(\text{SnD})$ (reduced units)	$K(\text{SnH})$ (reduced units)	$K(\text{SnD})$ (reduced units)
SnH_3^-	24.09 ± 0.01		24.09	
SnH_2D^-	24.76 ± 0.02	27.09 ± 0.14	24.76	27.08
SnHD_2^-	25.40 ± 0.03	27.72 ± 0.22	25.43	27.75
SnD_3^-		28.53 ± 0.43		28.42

property. In polyatomic molecules, there are usually several electronic factors of comparable size that contribute to the isotope effects on J . For polyatomic molecules, if 1J is most sensitive to the bond length, the one-bond shifts can also be written in the same way as for diatomic molecules, with the terms such as $(\partial J/\partial \alpha)_e(\langle \Delta \alpha \rangle^* - \langle \Delta \alpha \rangle) + \dots$ being less important. 2J and 3J , on the other hand, are very sensitive to bond and torsion angles.⁶²

Let us consider SnH_4 as an example rather than CH_4 , since fairly large isotope effects on SnH coupling have been observed. The types of terms that contribute to the vibrationally averaged spin–spin coupling are the same as those that contribute to the proton shielding in CH_4 as given in equation (51):

$$\langle K(\text{SnH}_1) \rangle = K_e + P_r \langle \Delta r_1 \rangle + P_s (\langle \Delta r_2 \rangle + \langle \Delta r_3 \rangle + \langle \Delta r_4 \rangle) + \text{terms in } P_{rr}, P_{ss}, P_{rs}, P_{st}, P_{\alpha}, \text{ etc.} \dots \quad (70)$$

where the primary derivative is $P_r \equiv (\partial K(\text{SnH}_1)/\partial r_{\text{SnH}_1})_e$ and the secondary derivative is $P_s \equiv (\partial K(\text{SnH}_1)/\partial r_{\text{SnH}_2})_e$. If we let $d \equiv \langle \Delta r_{\text{SnH}} \rangle$ in SnH_4 and $d - \Delta \equiv \langle \Delta r_{\text{SnD}} \rangle$ in SnD_4 then $d \approx 1.780$ pm and $\Delta \approx 0.5161$ pm can be obtained for $r_e = 170$ pm using the method described in Section 3.1. K_e is the reduced coupling constant at the equilibrium molecular geometry. The leading terms are⁶

$$\text{SnH}_4: \quad \langle K(\text{SnH}) \rangle = K_e + (P_r + 3P_s)d + \dots \quad (71)$$

$$\text{SnH}_3\text{D}: \quad \langle K(\text{SnH}) \rangle = K_e + (P_r + 2P_s)d + P_s(d - \Delta) + \dots \quad (72)$$

$$\langle K(\text{SnD}) \rangle = K_e + P_r(d - \Delta) + 3P_s d + \dots \quad (73)$$

$$\text{SnH}_2\text{D}_2: \quad \langle K(\text{SnH}) \rangle = K_e + (P_r + P_s)d + 2P_s(d - \Delta) + \dots \quad (74)$$

$$\langle K(\text{SnD}) \rangle = K_e + (P_r + P_s)(d - \Delta) + 2P_s d + \dots \quad (75)$$

$$\text{SnHD}_3: \quad \langle K(\text{SnH}) \rangle = K_e + P_r d + 3P_s(d - \Delta) + \dots \quad (76)$$

$$\langle K(\text{SnD}) \rangle = K_e + (P_r + 2P_s)(d - \Delta) + P_s d + \dots \quad (77)$$

$$\text{SnD}_4: \quad \langle K(\text{SnH}) \rangle = K_e + (P_r + 3P_s)(d - \Delta) + \dots \quad (78)$$

From the above, we see that the primary isotope effect, the difference⁶³

$$\begin{aligned} \Delta_p \ ^1K(\text{Sn}^{2/1}\text{H}) &= |^1K(\text{SnD})|_{\text{SnH}_3\text{D}}^* - |^1K(\text{SnH})|_{\text{SnH}_4} \\ &= (428.21 \pm 0.14) - (429.19 \pm 0.02) \\ &\approx -P_r \Delta \end{aligned} \quad (79)$$

leads to $P_r \approx 1.90$ reduced units pm^{-1} . The primary isotope effect may also be taken from any of the differences

$|^1K(\text{SnD})|_{\text{SnH}_2\text{D}_2} - |^1K(\text{SnH})|_{\text{SnH}_3\text{D}}$ or $|^1K(\text{SnD})|_{\text{SnHD}_3} - |^1K(\text{SnH})|_{\text{SnH}_2\text{D}_2}$ or $|^1K(\text{SnD})|_{\text{SnD}_4} - |^1K(\text{SnH})|_{\text{SnHD}_3}$, leading to an average value $P_r = (\partial K(\text{SnH}_1)/\partial r_{\text{SnH}_1})_e \approx 2.00$ reduced units pm^{-1} . Note that at this level of approximation, only the primary derivative P_r is involved in the primary isotope effect.

At the same time, the difference

$$\begin{aligned} \Delta_s \ ^1K(\text{SnH})[^{1/2}\text{H}] &= |K(\text{SnH})|_{\text{SnH}_3\text{D}}^* - |K(\text{SnH})|_{\text{SnH}_4} \\ &= (428.81 \pm 0.02) - (429.19 \pm 0.02) \\ &\approx -P_s \Delta \end{aligned} \quad (80)$$

leads to $P_s \approx 0.74$ reduced units pm^{-1} . Since this secondary isotope effect may be taken from three other differences such as $|^1K(\text{SnH})|_{\text{SnH}_2\text{D}_2} - |^1K(\text{SnH})|_{\text{SnH}_3\text{D}}$, etc., we get an average value $P_s = (\partial K(\text{SnH}_1)/\partial r_{\text{SnH}_2})_e \approx 0.75$ reduced units pm^{-1} and $K_e = 421.63$ reduced units. The primary isotope effect involves largely the primary derivative of the coupling constant, and the secondary isotope effect on the coupling involves largely the (secondary) derivative of the coupling constant with respect to stretching a remote bond.

We can do the same analysis for the isotopomers of SnH_3^- , and we find that the values $P_r = -5.80$ reduced units pm^{-1} , $P_s = -1.30$ reduced units pm^{-1} , and $K_e = 39.04$ reduced units reproduce the experimental values reasonably well, as seen in Table 10.

The agreement with the six experimental numbers is very good. These quantities can be translated back to Hz pm^{-1} as in Table 11.

It is interesting that, although the magnitude of the SnH coupling constant is about one order of magnitude smaller in SnH_3^- than in SnH_4 , the sensitivity of the spin–spin coupling to bond extension is almost three times as great. The lone pair is generally known to be responsible for negative contributions to the reduced coupling, leading to a much smaller magnitude of the spin–spin coupling. Apparently, it is also the lone pair (on Sn in SnH_3^-) that is responsible for the greater sensitivity to bond extension. By similar procedures, the changes in the reduced coupling constant with extension of the bond, $(\partial K/\partial r)_e$, or of an adjacent bond, $(\partial K/\partial r')_e$, can be estimated in other systems such as SnH_3^+ , PH_4^+ , PH_3 , PH_2^- , and SeH_2 from experimental values of $J(\text{AH})$ and

Table 11

	SnH_4	SnH_3^-
$(\partial J(\text{SnH})/\partial r)_e$ (Hz pm^{-1})	-9.00	+26.00
$(\partial J(\text{SnH})/\partial r')_e$ (Hz pm^{-1})	-3.40	+5.80
$\langle J(\text{SnH}) \rangle - J_e$ (Hz)	-34.1	+67.3
J_e (Hz)	-1899.3	-175.8

Table 12 Derivatives of the Reduced Spin–Spin Coupling Constant with Respect to Extension of the Bond Between the Coupled Nuclei (r) and With Respect to Extension of the Other Bond (r')⁶

Molecule	Empirical		Theoretical	
	$(\partial K/\partial r)_e$ (reduced units pm ⁻¹)	$(\partial K/\partial r')_e$ (reduced units pm ⁻¹)	$(\partial K/\partial r)_e$ (reduced units pm ⁻¹)	$(\partial K/\partial r')_e$ (reduced units pm ⁻¹)
Without lone pairs:				
HD			+1.4979	
CH ₄			+0.973 24	+0.5884
PH ₄ ⁺	+1.04 ± 0.20	+0.075 ± 0.02		
SnH ₄	+2.00 ± 0.30	+0.75 ± 0.07		
SnH ₃ ⁺	+6.00 ± 4.00	≈0		
With lone pairs:				
¹³ C ¹⁷ O			negative	
¹⁴ N ¹⁵ N			negative	
HF			-0.5156	
PH ₃	-4.22	+0.465		
PH ₂ ⁻	-1.25	-0.26		
SeH ₂	-1.90 ± 0.60	-0.71 ± 0.09		
SnH ₃ ⁻	-5.80 ± 0.40	-1.30 ± 0.10		

$J(\text{AD})$ combined with values of the dynamic factor calculated by the methods described in Section 3.1. These values are compared with some published theoretical values in Table 12. Since all are expressed as γ -free reduced coupling constants, these are purely electronic quantities, which can be directly compared with each other in sign and magnitude. Theory has shown that the Fermi contact term is most sensitive to bond stretch.^{64,65} Thus, it is not surprising that the magnitudes of the empirical derivatives in Table 12 increase with increasing spin density at the nucleus, just as the reduced coupling constants are known to do. The secondary derivative is generally smaller than the primary derivative, and both usually have the same sign. The earlier prediction by Jameson and Osten⁴ that $(\partial K(\text{AH})/\partial r)_e$ will generally be negative when A has lone pairs but will be positive otherwise appears to be correct.

In summary, the electronic factor in the one-bond coupling constant $(\partial K(\text{AH})/\partial r_{\text{AH}})_e$ has been found to have the following attributes that explain the observed trends.

1. For A without lone pairs, it is positive; that is, the magnitude of the coupling increases as the bond becomes stretched.
2. It is largely dominated by the Fermi contact term, which is very sensitive to the distance between the two nuclei, much more so than the spin–dipolar and orbital contributions to coupling.
3. Probably because of the dominance of the Fermi contact term, it is larger for nucleus A having larger atomic number.
4. For A with lone pairs, this electronic factor is negative. It is known that lone pairs make negative contributions to the spin–spin coupling. The sign of this electronic factor confirms that the lone pair contributions are very sensitive to bond extension.
5. The secondary electronic factor $(\partial K(\text{AH})/\partial r_{\text{AX}})_e$ is generally 2–5 times smaller than the primary electronic factor, and is a measure of the sensitivity of the coupling across one bond to the lengthening of another bond involving one of the coupled atoms.

In summary, the dynamic factors and electronic factors in isotope effects on NMR parameters have been characterized. The theoretical model is general for any molecular electronic property.²⁶ The effects can be completely understood within

the context of the Born–Oppenheimer approximation. Complete calculations can be carried out for individual molecules within this theoretical framework. Where such calculations have been carried out, the agreement with experiment is good. Under conditions where the leading terms are dominant, the molecule-specific higher order terms can be neglected so as to find explanations for and make predictions of the sweeping generalities that have surfaced empirically in isotope effects on NMR parameters. The dynamic factor that has been derived by assuming dominance of the bond stretching successfully predicted the mass dependence of the isotope effects observed later. The empirical electronic factors deduced from this model are found to be consistent (in sign, in magnitude, and in correlations with various quantities such as net charge, presence or absence of lone pairs, bond order, etc.) with the theoretical electronic factors obtained by ab initio calculations.

7 RELATED ARTICLES

Chemical Shift Scales on an Absolute Basis; Gas Phase Studies of Intermolecular Interactions and Relaxation.

8 REFERENCES

1. H. Batiz-Hernandez and R. A. Bernheim, in *Progress in Nuclear Magnetic Resonance Spectroscopy*, eds. J. W. Emsley, J. Feeney, and L. H. Sutcliffe, Pergamon Press, Oxford, 1967, Vol. 3, p. 63
2. P. E. Hansen, in *Annual Reports on NMR Spectroscopy*, ed. G. A. Webb, Academic Press, London, 1983, Vol. 15, p. 105.
3. P. E. Hansen, in *Progress in Nuclear Magnetic Resonance Spectroscopy*, eds. J. W. Emsley, J. Feeney, and L. H. Sutcliffe, Pergamon Press, Oxford, 1988, Vol. 20, p. 207.
4. C. J. Jameson and H. J. Osten, *J. Am. Chem. Soc.*, 1986, **108**, 2497.
5. C. J. Jameson and H. J. Osten, in *Annual Reports on NMR Spectroscopy*, ed. G. A. Webb, Academic Press, London, 1986, Vol. 17, p. 1.

6. C. J. Jameson, in *Isotopes in the Physical and Biomedical Sciences*, eds. E. Buncl and J. R. Jones, Elsevier, Amsterdam, 1991, Vol. 2, p. 1.
7. W. Gombler, *J. Am. Chem. Soc.*, 1982, **104**, 6616.
8. C. J. Jameson, *J. Chem. Phys.*, 1977, **66**, 4983.
9. R. Maple, J. E. Carson, and A. Allerhand, *J. Am. Chem. Soc.*, 1989, **111**, 7293.
10. J. R. Wesener, D. Moskau, and H. Gunther, *J. Am. Chem. Soc.*, 1985, **107**, 7307.
11. C. H. Arrowsmith, L. Baltzer, A. J. Kresge, M. F. Powell, and Y. S. Tang, *J. Am. Chem. Soc.*, 1986, **108**, 1356.
12. R. E. Wasylshen, J. O. Friedrich, S. Mooibroek, and J. B. Macdonald, *J. Chem. Phys.*, 1985, **83**, 548.
13. C. J. Jameson, A. K. Jameson, and D. Oppusunggu, *J. Chem. Phys.*, 1986, **85**, 5480.
14. M. Hoch and D. Rehder, *Inorg. Chim. Acta*, 1986, **111**, L13.
15. R. E. Wasylshen and N. Burford, *Can. J. Chem.*, 1987, **65**, 2707.
16. A. K. Jameson and C. J. Jameson, *J. Magn. Reson.*, 1978, **32**, 455.
17. R. E. Wasylshen and J. O. Friedrich, *Can. J. Chem.*, 1987, **65**, 2238.
18. B. Bennett and W. T. Raynes, *Spectrochim. Acta A*, 1989, **45**, 1267.
19. C. J. Jameson and H. J. Osten, *J. Chem. Phys.*, 1984, **81**, 4293.
20. N. F. Ramsey, *Phys. Rev.*, 1952, **87**, 1075.
21. C. J. Jameson, *J. Chem. Phys.*, 1977, **66**, 4977.
22. C. J. Jameson, A. K. Jameson, and S. M. Cohen, *J. Chem. Phys.*, 1977, **67**, 2771.
23. A. K. Jameson, K. Schuett, C. J. Jameson, S. M. Cohen, and H. Parker, *J. Chem. Phys.*, 1977, **67**, 2821.
24. C. J. Jameson, *Bull. Magn. Reson.*, 1980, **3**, 3.
25. C. J. Jameson, *Chem. Rev.*, 1991, **91**, 1375.
26. C. J. Jameson, in *Theoretical Models of Chemical Bonding*, ed. Z. B. Maksic, Springer-Verlag, Berlin, 1991, Part 3, p. 457.
27. C. J. Jameson and H. J. Osten, *J. Chem. Phys.*, 1984, **81**, 4300.
28. C. J. Jameson and A. K. Jameson, *J. Chem. Phys.*, 1986, **85**, 5484.
29. D. R. Herschbach and V. W. Laurie, *J. Chem. Phys.*, 1961, **35**, 458.
30. R. A. Hegstrom, *Phys. Rev. A*, 1979, **19**, 17.
31. C. J. Jameson and A. C. de Dios, *J. Chem. Phys.*, 1993, **98**, 2208.
32. R. Ditchfield, *Chem. Phys.*, 1981, **63**, 185.
33. D. B. Chesnut and C. K. Foley, *J. Chem. Phys.*, 1986, **84**, 852.
34. D. B. Chesnut and D. W. Wright, *J. Comput. Chem.*, 1991, **12**, 546.
35. A. C. de Dios and C. J. Jameson, in *Annual Reports on NMR Spectroscopy*, ed. G. A. Webb, Academic Press, London, 1994, vol. 29, p. 1.
36. C. J. Jameson, A. C. de Dios, and A. K. Jameson, *J. Chem. Phys.*, 1991, **95**, 1069.
37. G. Riley, W. T. Raynes, and P. W. Fowler, *Mol. Phys.*, 1979, **38**, 877.
38. A. R. Hoy, I. M. Mills, and G. Strey, *Mol. Phys.*, 1972, **24**, 1265.
39. M. Toyama, T. Oka, and Y. Morino, *J. Mol. Spectrosc.*, 1964, **13**, 193.
40. W. T. Raynes, P. W. Fowler, P. Lazzeretti, R. Zanasi, and M. Grayson, *Mol. Phys.*, 1988, **64**, 143.
41. P. W. Fowler, G. Riley, and W. T. Raynes, *Mol. Phys.*, 1981, **42**, 1463.
42. C. J. Jameson, A. C. de Dios, and A. K. Jameson, *J. Chem. Phys.*, 1991, **95**, 9042.
43. W. T. Raynes, *Mol. Phys.*, 1988, **63**, 719.
44. P. W. Fowler and W. T. Raynes, *Mol. Phys.*, 1981, **43**, 65.
45. C. J. Jameson, in *Specialist Periodical Reports on NMR*, ed. G. A. Webb, Royal Society of Chemistry, London, 1989, Vol. 19, p. 1.
46. J. A. Tossell and P. Lazzeretti, *J. Magn. Reson.*, 1988, **80**, 39.
47. R. E. Wasylshen, *Can. J. Chem.*, 1982, **60**, 2194.
48. H. J. Osten and C. J. Jameson, *J. Chem. Phys.*, 1985, **81**, 4288.
49. H. J. Osten and C. J. Jameson, *J. Chem. Phys.*, 1985, **82**, 4595.
50. J. O. Friedrich and R. E. Wasylshen, *J. Chem. Phys.*, 1985, **83**, 3707.
51. C. J. Jameson and H. J. Osten, *J. Chem. Phys.*, 1984, **81**, 2556.
52. D. B. Chesnut, *Chem. Phys.*, 1986, **110**, 415.
53. P. Lazzeretti, R. Zanasi, A. J. Sadlej, and W. T. Raynes, *Mol. Phys.*, 1987, **62**, 605.
54. C. J. Jameson and H. S. Gutowsky, *J. Chem. Phys.*, 1964, **40**, 1714.
55. C. J. Jameson and J. Mason, in *Multinuclear Nuclear Magnetic Resonance*, ed. J. Mason, Plenum Press, London, 1987, p. 51.
56. C. J. Jameson and H. J. Osten, *J. Am. Chem. Soc.*, 1985, **107**, 4158.
57. C. J. Jameson, *Mol. Phys.*, 1985, **54**, 73.
58. A. A. Borisenko, N. M. Sergeev, and Y. A. Ustynyuk, *Mol. Phys.*, 1971, **22**, 715.
59. M. Alei and W. E. Wageman, *J. Chem. Phys.*, 1978, **68**, 783.
60. T. Schaefer, J. Peeling, and R. Sebastian, *Can. J. Phys.*, 1987, **65**, 534.
61. H. J. Jakobsen, A. J. Zozulin, P. D. Ellis, and J. D. Odom, *J. Magn. Reson.*, 1980, **38**, 219.
62. W. T. Raynes, J. Geertsen, and J. Oddershede, *Chem. Phys. Lett.*, 1992, **197**, 516.
63. K. L. Leighton and R. E. Wasylshen, *Can. J. Chem.*, 1987, **65**, 1469.
64. J. Oddershede, J. Geertsen, and G. Scuseria, *J. Phys. Chem.*, 1988, **92**, 3056.
65. J. Geertsen, J. Oddershede, and G. E. Scuseria, *J. Chem. Phys.*, 1987, **87**, 2138.

Biographical Sketch

Cynthia J. Jameson. b 1937. B.S., University of the Philippines; Ph.D., 1963, University of Illinois at Urbana-Champaign. Introduced to NMR by Herb Gutowsky. Faculty in Chemistry, University of Illinois at Chicago, 1968–present. Approx. 130 publications. Research interests include theoretical and experimental studies of the chemical shift in simple systems in the gas phase and in molecules adsorbed in microporous solids, with particular emphasis on intramolecular and intermolecular shielding surfaces and averages therein; also, spin relaxation in gases and their connection with the anisotropy of intermolecular potentials and molecular dynamics.